



TITLE:

Abstracts of the Papers Published by the
Staff Members of the Institute from July,
1975 to June, 1976 (Special Issue on the
Commemoration of the Fiftieth Anniversary)

AUTHOR(S):

CITATION:

Abstracts of the Papers Published by the Staff Members of the Institute from July, 1975 to June, 1976 (Special Issue on the Commemoration of the Fiftieth Anniversary). Bulletin of the Institute for Chemical Research, Kyoto University 1977, 54(6): 472-518

ISSUE DATE:

1977-03-25

URL:

<http://hdl.handle.net/2433/76686>

RIGHT:

Abstracts of the Papers Published by the
Staff Members of the Institute from
July, 1975 to June, 1976

Nuclear Chemistry

Further Remarks on the Total Probability of K -Electron Shake-Off in Beta Decay. Y. Iozumi and S. Shimizu. *Lettere al Nuovo Cimento*, **13**, 422 (1975).—The total beta decay rate is evaluated in the following model: two electrons are bound in the K -shell of the parent atom with nuclear charge Z , and in the final state three electrons (two atomic and one nuclear) can make transitions to bound or continuum states of the daughter atom with $Z+1$. The rates due to the K electron shake-off and K electron shake-up can be expressed as small portions of the total decay rate. Results are compared with calculations of Law and Campbell.

Time-Filtering Effect in the Mössbauer Spectrum. T. Kobayashi and S. Shimizu. *Phys. Letters*, **54A**, 311 (1975).—Details of the delayed-coincidence transmission Mössbauer spectra have been observed using a ^{57}Co source in copper and a single-line absorber $\text{K}_4\text{Fe}(\text{CN})_6 \cdot 3\text{H}_2\text{O}$, for fairly narrow predetermined delayed time intervals. A very good agreement was found between the experimental results and theoretical predictions.

Internal Ionization Accompanying K Conversion: One-Step Theory. T. Mukoyama and S. Shimizu. *Phys. Rev. C*, **13**, 377 (1976).—A one-step theory of internal ionization accompanying K conversion has been developed. The ionization probability and the energy spectrum of the ejected electrons have been calculated using screened relativistic hydrogenic wave functions. It is shown that the probabilities calculated using the present model are in good agreement with the recent experimental values for the K -shell internal ionization accompanying K conversion. The calculated results predict that the ionization probability is dependent on the nuclear transition energy and on the multipolarity of the transition. The multipolarity dependence of the spectral shape of the ejected electrons has also been studied.

[RADIOACTIVITY ^{57}Fe , $^{95,96}\text{Mo}$, ^{97}Tc , ^{109}Ag , $^{113,114}\text{In}$, ^{131}Xe , ^{137}Ba , ^{141}Pr , ^{150}Sm , ^{169}Tm , ^{203}Tl ; calculated internal ionization probability accompanying K conversion, ejected-electron spectrum.]

Comments on the Recent Theory of K -Electron Shake-Off in Beta-Decay. Y. Iozumi and S. Shimizu. *Lettere al Nuovo Cimento*, **14**, 193 (1975).—In order to resolve an argument concerning K -electron shake-off in beta decay, an elementary mistake in a previous formulation with the second-quantization description is directly revealed.

Double K -Hole Creation in the Decay of ^{137m}Ba . S. Ito, Y. Isozumi, and S. Shimizu. *Bull. Inst. Chem. Res., Kyoto Univ.*, **54**, 23 (1976).—Double K -hole creation in the decay of ^{137m}Ba has been studied by means of two Si(Li) detectors for two K X rays emitted when the double K hole is filled and an anthracene crystal with 4π -detection geometry for electrons from a ^{137}Cs source. The total probability per K conversion, that the double K hole is formed, has been determined to be less than 10^{-4} . The comparison of the present result with existing theories and also with previous experimental results is given.

Measurement of Ion Current by a Conventional Sampling Method. R. Katano, S. Kakiuchi, and H. Mazaki. *Bull. Inst. Chem. Res., Kyoto Univ.*, **54**, 30 (1976).—Precise measurements of ion current of 10^{-10} – 10^{-13} A produced in an ionization chamber by radioactive sources have been attempted by means of a conventional sampling method. By the use of a vibrating-reed electrometer (VRE), a digital multimeter (DMM), and a multi-channel analyzer (MCA) in multi-channel scaling (MCS) mode, it was found that the ion current can be determined within experimental errors of 0.03%.

Determination of Decay Constant by the Maximum Likelihood Method. T. Mukoyama. *Bull. Inst. Chem. Res., Kyoto Univ.*, **54**, 48 (1976).—A method for analysis of decay data is presented. The method is based on maximum likelihood theory and so general that it is applicable to any other experimental distributions. The validity of the proposed method has been successfully tested against the artificial decay data. It is pointed out that the present method is more simple than the previous maximum likelihood methods.

Tabulated Values Used for Radiation Shielding against γ Rays from Radioisotopes. T. Mukoyama. *Bull. Inst. Chem. Res., Kyoto Univ.*, **54**, 54 (1976).—Tables that are suitable for calculations of radiation shielding against point isotropic γ -ray sources have been generated by spline interpolation from the recent data. As γ -ray sources, the common radioisotopes are considered and interpolation has been made for the major γ -ray energies of these nuclides.

Values of the energy absorption coefficients for air are obtained and the R_{hm} values of these nuclides are calculated. Table of the total attenuation coefficients is presented for six materials of interest. The dose buildup factors are approximated by the Berger's two-parameter formula. Tables of the coefficients of the Berger function are given for five shielding materials.

Range of Electrons and Positrons. T. Mukoyama. *Nucl. Instr. & Meth.*, **134**, 125 (1976).—The range of electrons and positrons in detector materials has been calculated by the Wilson theory. The results obtained are compared with the values estimated from the continuous-slowning-down model. A correction factor which depends only on the energy is presented. It is concluded that the corrected Wilson theory yields good approximate values for ranges of electrons and positrons in the energy region above 70 keV.

Double K -Hole Creation in the Internal Conversion Decays of ^{141}Pr and $^{137\text{m}}\text{Ba}$. S. Ito, Y. Isozumi, and S. Shimizu. *Abstracts of Contributed Papers, The Second International Conference on Inner Shell Ionization Phenomena, March 29–April 2, 1976*, 174 (1976).—The double K -hole creation process in the internal conversion decay has been studied experimentally for the 145-keV M1 transition of ^{141}Pr and the 662-keV M4 transition of $^{137\text{m}}\text{Ba}$. The coincidence measurements were performed between two K x rays emitted when the double K vacancy is filled, using two high-resolution Si(Li) detectors. Preliminary values of the total probability per K conversion (P_{KK}), that the double K vacancy is formed, are $(4 \pm 2) \times 10^{-5}$ for Pr and $< 5 \times 10^{-5}$ for Ba.

Another Possible Origin of K -Shell Internal Ionization and Excitation in β Decay. Y. Isozumi, S. Shimizu, and T. Mukoyama. *Abstracts of Contributed Papers, The Second International Conference on Inner Shell Ionization Phenomena, March 29–April 2, 1976*, 179 (1976).—The re-formulation of the K -shakeoff probability of the internal ionization in β decay by correcting the mistake in the theory of Law and Campbell is presented. The noteworthy disagreement between our calculated values and recent experimental data may be due to neglecting an important effect in the present calculations, the Coulomb interaction between β particle and emitted K electron in the final state.

Many-Electron Effect on the K -Shell Internal Ionization Accompanying β^- Decay. T. Mukoyama and S. Shimizu. *Abstracts of Contributed Papers, The Second International Conference on Inner Shell Ionization Phenomena, March 29–April 2, 1976*, 182 (1976).—The many-electron effect has been taken into account when the theoretical treatment of the K -shell internal ionization during β^- decay was developed. Basing upon the newly developed treatment the K -shell ionization probability are calculated for seven nuclides. The comparison of the present model with the hydrogenic model indicates that many-electron effect substantially increases the probability.

Multiparameter Data Acquisition System with a Mini-Computer. T. Miyana, T. Ohsawa, S. Tanaka, N. Fujiwara, S. Kakigi, K. Fukunaga, and T. Yanabu. *Bull. Inst. Chem. Res., Kyoto Univ.*, **52**, 1 (1976).—Multiparameter data acquisition system with a YHP 2100A computer was developed. Details of hardware and outlines of softwares are described. This system is now used as 3 parameter system, but expandable to 4 or more parameter system. The system is very useful for multi-particle coincidence experiment such as three body reaction. An example is shown for the detection of elastic scattering between protons and deuterons.

The (^3He , ^3He), (^3He , $^3\text{He}'$), and (^3He , α) Reactions on ^{12}C at 82.1 MeV. T. Tanabe, K. Koyama, M. Yasue, H. Yokomizo, K. Sato, J. Kokame, N. Koori, and S. Tanaka. *J. Phys. Soc. Japan*, **41**, 361 (1976).—The nucleus ^{12}C was bombarded by 82.1-MeV ^3He particles to study elastic and inelastic scattering and the (^3He , α) reaction. Angular distributions were measured for the elastic scattering, for the inelastic scattering to levels at 4.4, 7.6, and 9.6 MeV in ^{12}C , and for the (^3He , α) reaction to 0.0, 2.0, 4.3 (4.7), and 6.4 MeV in ^{12}C . The optical potential parameters were

searched for to fit the ^3He elastic scattering angular distribution. The deformation parameters β_2 and β_3 for ^{12}C were determined from DWBA analysis. The angular distributions of α particles were compared with DWBA calculations and calculations including the two-step process via inelastic channel.

On the Final-State Interactions in (e, e'p) Reactions. K. Nakamura and N. Izutsu. *Nuclear Phys. A*, **A259**, 301 (1976).—Distorted momentum distributions in the ^{12}C (e, e'p) reaction are calculated using the Elton-Swift wave functions for the bound-state protons. Final-state interactions between the ejected proton and residual nucleus are taken into account by means of the WKB approximation using the complex optical potential. It is shown that the factors governing qualitative features of the distorted momentum distributions are the angle ω between the recoil momentum vector and the vector \mathbf{k}_p and the quantity $(E_p/\mathbf{k}_p) \text{Re } \bar{V}$, where (E_p, \mathbf{k}_p) is the four momentum of the ejected proton and $\text{Re } \bar{V}$ is some average value of the real part of the optical potential. Measurement of the distorted momentum distributions over a wide range of the angle ω is proposed.

$^4\text{He}(p, 2p) ^3\text{He}$ and $^4\text{He}(p, pd)^3\text{H}$ Reactions at 156 MeV. R. Frascaria, P. G. Roos, M. Morlet, N. Marty, A. Willis, V. Comparat, and N. Fujiwara. *Phys. Rev. C*, **12**, 243 (1975).—Quasifree proton-proton and proton-deuteron scattering cross section on ^4He have been measured and compared with theoretical calculations in the distorted wave impulse approximation. Information on the low components for the proton and deuteron momentum distributions in ^4He are deduced.

Elastic Proton Scattering on ^4He at 156 MeV. V. Comparat, R. Frascaria, N. Fujiwara, N. Marty, M. Morlet, P. G. Roos, and A. Willis. *Phys. Rev. C*, **12**, 251 (1975).—The differential cross section for the proton ^4He elastic scattering at 156 MeV was measured in the angular range from 10° to 168° . An optical potential analysis with an exchange term is performed and extended to the 100 and 85 MeV data. Some of the impulse approximations are tested and a comparison is performed with a Glauber calculation.

Proton-induced ^3He breakup at 156 MeV. J. P. Didelez, R. Frascaria, N. Fujiwara, I. D. Goldman, E. Hourany, H. Nakamura-Yokota, F. Reide, and T. Yuasa. *Phys. Rev. C*, **12**, 1974 (1975).—The ^3He breakup induced by a 156 MeV proton beam was studied using a liquid target and the adequate kinematic conditions for p - p , p - n , and p - d quasifree scattering or three nucleon final state interactions. The $(p, 2p)$ and (p, pn) differential cross section spectra ($d^3\sigma$) are similar to each other for recoil energy less than 10 MeV and coincide to those calculated with a plane-wave impulse approximation. The $d^3\sigma$ spectrum of the (p, pd) reaction shows a peak at the minimum p - d relative energy indicating their final state interaction.

Analytical Chemistry

Coprecipitation Behavior of Zinc in the Oxygenation Process of Ferrous

Iron. T. Shigematsu, T. Ōmori, T. Aoki, and M. Matsui. *Bull. Inst. Chem. Res., Kyoto Univ.*, **53**, 435 (1975).—To understand the fixation of metal ions in soils and water, the coprecipitation of zinc and cobalt with hydrous ferric oxide generated in the oxygenation process of ferrous ion was investigated. As a preliminary experiment, several oxygenation reactions of ferrous ion ran at various pH values by bubbling oxygen gas or air. The rate of oxygenation was the first order with respect to Fe(II). The over-all rate constant, k , at 25°C was found to be 2.7×10^{13} liter² mole⁻² atm⁻¹ min⁻¹ in case of the oxygen bubbling.

The coprecipitation of zinc was scarcely affected by the zinc concentration in the parent solution. This shows that zinc ion is not adsorbed on the surface of hydrous ferric oxide but is distributed between the hydrous ferric oxide and the parent solution. Zinc ion was found to be coprecipitated in the hydrous ferric oxide obeying the Doerner and Hoskins logarithmic distribution law, judging from the four possible distribution coefficients calculated. Distribution and adsorption phenomena seem to exist together in the coprecipitation of cobaltous ion, considering some dependency of pH and cobalt concentration on the coprecipitated amount.

Coprecipitation of Lead with Hydroxyapatite. O. Fujino, M. Matsui, and T. Shigematsu. *Bull. Inst. Chem. Res., Kyoto Univ.*, **53**, 444 (1975).—The distribution behavior of lead between aqueous phase and hydroxyapatite was investigated. Hydroxyapatite precipitates were prepared by dropping hydrogenphosphate ion extremely slowly to an aqueous solution containing calcium, lead, ethylenediamine, and glycine at 80°C. The lead ion was coprecipitated in the apatite, obeying the Doerner and Hoskins logarithmic distribution law. Apparent distribution coefficient was roughly constant, though the stability constants at room temperature were used in calculating them. That the distribution coefficient of lead has a high value, approximately $10^{7.3}$, shows its high affinity for such apatite minerals as mineral bone.

Coprecipitation of Cadmium with Hydroxyapatite. O. Fujino. *Bull. Inst. Chem. Res., Kyoto Univ.*, **53**, 464 (1975).—The distribution behavior of the cadmium ion between hydroxyapatite precipitates and aqueous solution phase was studied, where the hydroxyapatite was prepared by the extremely slow addition of diammonium hydrogenphosphate to the solutions of cadmium and calcium nitrates buffered with ethylenediamine at 80°C. The cadmium ion was coprecipitated in the hydroxyapatite, obeying the Doerner and Hoskins logarithmic distribution law. Apparent distribution coefficient was remarkably affected by the ethylenediamine concentration and the pH value. The true distribution coefficient, λ^0 , was calculated by using the stability constants of proton and cadmium ion with ethylenediamine at 80°C, and its value gave a constant, about $10^{3.4}$, independently of the ethylenediamine amount and the pH value.

Fluorometry. T. Shigematsu. *Bunseki*, **6**, 348 (1976), in Japanese.—Review.

Activation Analysis of Trace Metals in Water and Dust. T. Shigematsu. *Kagaku (Chemistry)*, **31**, 62 (1975), in Japanese.—Review.

Determination Copper in Sea Water and Shellfishes by Atomic Absorption Spectrometry with a Carbon Tube Atomizer. T. Shigematsu, M. Matsui, O. Fujino, S. Mitsuno, and T. Nagahiro. *Nippon Kagaku Kaishi (J. Chem. Soc. Japan, Chem. Ind. Chem.)* 1328 (1975), in Japanese.—Atomic absorption spectrometry using a carbon tube atomizer was used for the determination of copper in sea water and sea water clam, and simultaneously the investigations of the applied carbon tube temperature (voltage), argon flow rate, calibration curve, and the interference of diverse ions were carried out.

A constant absorption signal was observed at a carbon tube temperature (voltage) of above *ca.* 2000°C (7 V). In the present determination the carbon tube atomizer was operated at a temperature (voltage) of *ca.* 2500°C (8 V).

A constant absorbance of copper was observed at a lower argon flow rate than 2ℓ/min. However, when the argon flow rate became higher than 2ℓ/min, absorbance of copper decreased, but the reproducibility of absorbance was excellent.

In the range of $(2.5\sim 15) \times 10^{-10}$ g of copper, a fairly linear calibration curves were obtained by the injection of 10 μℓ of the copper solution whose concentrations were 0.025~0.15 ppm. The sensitivity (1% absorption was 4×10^{-11} g and R.S.D. was 2.8 per cent.

The effect of salts on the peak absorbance of copper was studied with regard to the solution of copper (0.2 ppm) containing 100 or 1000 fold excess of salts. For 1000 fold excess, most salts interfered with it.

Copper content in sea water and sea water clam was determined by extracting copper into diisobutyl ketone as diethyldithiocarbamate. By this method, concentrations of copper in sea water, shell and soft tissues of the clam were found to be 0.0036~0.014, 0.15~0.38, and 0.43~8.3 ppm, respectively. In the soft tissue such as liver, kidney, and labial palps copper was found to be somewhat enriched.

Physical Chemistry

On the Dielectric Relaxation in Ferrites due to Electron Hopping at Low Temperatures. K. Iwauchi, N. Koizumi, M. Kiyama, and Y. Bando. *Bull. Inst. Chem. Res., Kyoto Univ.*, **52**, 596 (1974).—Dielectric dispersions were found in the powder samples of Fe_3O_4 , $\text{Mn}_{1.4}\text{Fe}_{1.6}\text{O}_4$, $\text{Mn}_{0.8}\text{Fe}_{2.2}\text{O}_4$, $\text{Zn}_{0.6}\text{Fe}_{2.4}\text{O}_4$, and $\text{Mn}_{0.59}\text{Zn}_{0.33}\text{Fe}_{2.08}\text{O}_4$ at temperatures from 77 to 4.2 K. The dielectric relaxations were connected with the existence of Fe^{2+} ions and the magnitudes of dielectric dispersion were roughly proportional to the amounts of Fe^{2+} ions in the samples. The activation energies obtained from the temperature dependences of electrical conductivity were close to those obtained from dielectric relaxation. The dielectric relaxation was considered to be caused by the hopping of electron between Fe^{2+} and Fe^{3+} ions on the octahedral sites in the spinel structure.

Numerical Estimation in a Theory of Interfacial Polarization Developed for Disperse Systems in High Concentrations. T. Hanai and N. Koizumi. *Bull. Inst. Chem. Res., Kyoto Univ.*, **54**, 248 (1976).—Numerical calculations are carried

out to obtain solutions of a theoretical expression of interfacial polarization, which was proposed by Hanai [*Kolloid Z.*, **171**, 23 (1960)], applicable to concentrated disperse systems of spherical particles. It is found from the results that the dielectric relaxation characterized by the changes in the dielectric constants and the electrical conductivities extends over an apparently broader range of frequency in comparison with a single relaxation system, and that the complex plane plots of the complex dielectric constants show remarkable depression from a semicircle. Some comparisons of the limiting dielectric constants and electrical conductivities at low and high frequencies are made between the present results and those by approximate equations so far used. The relaxation frequency giving the maximum loss factor is found to be strongly dependent on the concentration of the disperse phase and to reduce to very low values at higher concentrations in conformity with experimental results.

Magnetic Relaxation in Fe_3O_4 and Ferrites. K. Iwauchi, N. Koizumi, M. Kiyama, and Y. Bando. *Bull. Inst. Chem. Res., Kyoto Univ.*, **54**, 255 (1976).—Magnetic permeability and loss tangent ($\tan \delta$) of Fe_3O_4 and some ferrites were measured in the frequency range of 100 kHz to 1 MHz and the temperature range of 4.2 to 300 K with a transformer bridge by using the three terminal method. While $\gamma\text{-Fe}_2\text{O}_3$ which has no Fe^{2+} ion showed no peak in $\tan \delta$ -T curve, Fe_3O_4 showed a peak in $\tan \delta$ near 40 K. MnZn ferrite with Fe^{2+} ions showed two peaks in $\tan \delta$ near 30 and 150 K. The peak near 30 K was considered to be caused by the hopping of electron between Fe^{2+} and Fe^{3+} ions and the peak near 150 K by the electronic process of Mn ions.

Remarks on the Hamon Approximation. Y. Kita and N. Koizumi. *Advan. Mol. Relaxation Processes*, **7**, 13 (1975).—The accuracy of the Hamon approximation for evaluating the dielectric loss, the relaxation time, and the relaxation intensity from transient absorption current data was discussed with regard to dielectric relaxations of the Cole–Cole, Davidson–Cole and Williams–Watts type. It was found that the Hamon approximation enables us to evaluate the relaxation intensity and the dielectric loss, at frequencies higher than the relaxation frequency, with good accuracy, regardless of the type of relaxation, but it introduces significant errors in calculations of the dielectric loss at lower frequencies and in the relaxation time, particularly in relaxations of the Davidson–Cole type and other types with a narrow distribution of relaxation times. The approximation is applicable, with fairly good accuracy, to the Cole–Cole type of relaxation with a broad distribution of relaxation times.

Dielectric Properties of Synaptosomes Isolated from Rat Brain Cortex. A. Irimajiri, T. Hanai, and A. Inouye. *Biophys. Struct. Mechanism*, **1**, 273 (1975).—Dielectric measurements were performed on the suspensions of synaptosomes isolated from rat brain cortex. The synaptosomes in buffered salt media showed typical dielectric dispersions caused by the presence of a thin limiting membrane of sufficiently low conductivity. An analysis of the dielectric data revealed that the electric conductivity of the synaptosome interior was about 37% of the external medium conductivity under isotonic conditions and that the dielectric constant for the interior phase was about 35. The membrane capacitance ($0.7 \mu\text{F cm}^{-2}$) remained constant

irrespective of nature and concentration of the univalent salts examined. Significant reduction in both the conductivity and the dielectric constant of the internal phase can be explained theoretically provided that some intrasynaptosomal structure (synaptic vesicles and/or small mitochondria) of non-conducting nature occupies about 50% of the particulate volume, the remainder being in equilibrium with the external salt medium.

A Method for Determining the Dielectric Constant and the Conductivity of Membrane-Bounded Particles of Biological Relevance. T. Hanai, N. Koizumi, and A. Irimajiri. *Biophys. Struct. Mechanism*, **1**, 285 (1975).—Numerical assessment is made regarding Pauly and Schwan's theory which describes the dielectric behavior of a suspension of "shell spheres" as a model of biological membrane-bounded particles. The results indicate that approximate expressions of the theory may give rise to serious errors when applied to particles smaller than about $1\text{ }\mu\text{m}$ in diameter. With a view to performing analysis according to a general expression of the theory, some of the characteristic responses of dielectric parameters upon changes in phase parameters are examined with particular reference to some numerical ranges of biological interest. On this basis a simplified and systematic procedure is proposed for estimating the phase parameters of particles whose shell phase can be regarded as non-conductive. As the application of the procedure proposed, a set of dielectric data of a synaptosome suspension is analyzed, so that the following three phase parameters are successfully determined: membrane capacitance (or shell phase dielectric constant), internal phase conductivity and internal phase dielectric constant. Some limitations are discussed of the procedure for the cases of conducting shells and small particles.

Dielectric Properties of Yeast Cells. K. Asami, T. Hanai, and N. Koizumi. *J. Membrane Biol.*, **28**, 169 (1976).—Dielectric measurements were made on suspensions of intact yeast cells over a frequency range from 10 kHz to 100 MHz. The suspensions showed typical dielectric dispersions, which are considered to be caused by the presence of cytoplasmic membranes with a sufficiently low conductivity. Since the conductivity of the cell wall was found to be nearly the same values as that of the suspending medium composed of KCl solutions in a range from 10 mM to 80 mM, the cell wall may be ignored on establishing an electrical model of the cells suspended in such media. An analysis of the dielectric data was carried out by use of Pauly and Schwan's theory. The membrane capacitance was estimated to be $1.1 \pm 0.1\text{ }\mu\text{F}/\text{cm}^2$, which is compared with values reported so far for most of biological membranes. The conductivity of the cell interior was almost unchanged with varying KCl concentrations and showed low values owing to the presence of less conducting particles, presumably intracellular organelles. The relatively low dielectric constants of about 50 obtained for the cell interior in comparison with values of aqueous solutions may be attributed also to the presence of intracellular organelles and proteins.

Electron Micrographs of Lecithin Films. H. E. Ries, Jr., M. Matsumoto, and N. Uyeda. *Bull. Inst. Chem. Res., Kyoto Univ.*, **53**, 77 (1975).—Monolayers of a

synthetic lecithin transferred from a water surface to electron-microscope supports show a pronounced porous structure at low and intermediate pressures. The small holes and the irregular structure of the film may be related to a microporosity of cell membranes.

Orientation of Anthracene in Stretched Polyvinylchloride. N. Kimura and S. Hayashi. *Bull. Inst. Chem. Res., Kyoto Univ.*, **54**, 263 (1976).—Dichroic measurements were made of anthracene in polyvinylchloride films stretched at various degree of elongation. A band at 363 nm of anthracene shows parallel dichroism at small elongation, but perpendicular at large elongation. This change of dichroism was theoretically interpreted. The results indicate that the long axis and the plane of the anthracene molecule orients predominantly parallel to the stretching direction.

Electron Microscope Studies of Monolayers of Lecithin. H. E. Ries, Jr., M. Matsumoto, N. Uyeda, and E. Suito. *Advances in Chemistry Series*, **144**, 286 (1975).—Electron micrographs of the monolayers of a synthetic lecithin, β , γ -dipalmitoyl-DL- α -glycerylphosphorylcholine, are markedly different from those of fatty acids and cholesterol. However, the overall thin film properties of these materials, as indicated by pressure-area isotherms, are quite similar. At low surface pressure, the island structures of lecithin films are far less regular in contour than those of fatty acid or cholesterol films. The lecithin films also have an unusual microporosity. This perforated structure persists at intermediate and high pressures. After monolayer collapse, the long, flat, ribbonlike structures formed by lecithin are less regular than the well defined collapse structures of fatty acids and cholesterol. Such similarities and differences are related to molecular geometry and the location and strength of polar groups.

Infrared Spectroscopic Evidence for the Coexistence of Two Molecular Configurations in Crystalline Fatty Acids. S. Hayashi and J. Umemura. *J. Chem. Phys.*, **63**, 1732 (1975).—Infrared spectra of 14 normal fatty acids have been obtained in the range of temperatures from room temperature to liquid-helium temperature. Great temperature dependencies are observed in their spectra, especially in the region of the characteristic frequencies of the carboxyl group, and the band progression of the CH_2 wagging modes. Many bands decrease in intensity with decreasing temperature and disappear near liquid-helium temperature. Close to the positions of these lost bands, alternative bands, which increase in intensity with decreasing temperature, are found. The results support the postulate proposed in our earlier work that the two distinct configurations, *cis* and *trans* forms for $\text{C}_\beta-\text{C}_\alpha-\text{C}=\text{O}$ group, coexist in the crystalline state, and indicate that (1) the *cis* configuration is the lower energy (enthalpy) form for the odd acids (C_3-C_{11}) and the acids containing four or six carbon atoms; and (2) the *trans* configuration is lower energy form for the even-numbered (C_8-C_{20}) carbon series. Difference of enthalpy and entropy between *cis* and *trans* forms of $\text{CH}_3(\text{CH}_2)_{12}\text{COOH}$ are estimated to be about 200 cal/mole-deg, respectively.

Resonance Raman Spectra of Monolayers Adsorbed at the Interface between Carbon Tetrachloride and an Aqueous Solution of a Surfactant and a Dye. T. Takenaka and T. Nakanaga. *J. Phys. Chem.*, **80**, 475 (1976).—Resonance Raman spectra have been recorded of a monolayer adsorbed at the interface between carbon tetrachloride and an aqueous solution of cetyltrimethylammonium bromide (CTAB, a cationic surfactant) and methyl orange (MO, an anionic azo dye) by using a new method of total reflection of the exciting light at the interface. The adsorbed monolayer consisted of an interaction product of CTAB with MO, and the latter served as an absorber of the exciting light of an Ar⁺ laser to give rise to the resonance Raman effect. The band frequencies of MO in the monolayer were slightly shifted from those in bulk aqueous solution toward those of solid MO, indicating that the MO molecules in the monolayer were in an environment similar to a crystal field. Theoretical consideration of the Raman scattering activity due to an evanescent wave in the total reflection has been made of uniaxially oriented molecules. From polarization measurements of the resonance Raman spectra, it was found that the long axes of the MO molecules were tilted in the monolayer with a large angle of 50–60° with the axis normal to the interface.

Studies of Surface Chemistry by Means of Raman Spectroscopy. T. Takenaka. *Hyomen (Surface)*, **14**, 303 (1976), in Japanese.—With the development of the laser Raman spectrophotometer, it has been applying to the molecular studies of surface chemistry, because Raman spectroscopy possesses many advantages over infrared spectroscopy. Among those the fact that studies of aqueous solutions are much easier by the Raman spectroscopy than by the infrared spectroscopy is most significant. The application of the resonance Raman effect is also very useful in this field. This review article introduces papers dealing with Raman spectra of adsorbed species at various interfaces. Contents of the article are as follows:

1. Introduction.
 2. Advantages of Raman spectroscopy in studying surface chemistry.
 3. Adsorption at gas-solid interfaces.
 4. Adsorption on electrode surfaces.
 5. Thin layers on solid surfaces.
 6. Adsorbed monolayers at liquid-liquid interfaces.
 7. Postscript.
- References.

Isomerization of Chemically Activated 1-Buten-1-yl and 1-Buten-4-yl Radicals. T. Ibuki, A. Tsuji, and Y. Takezaki. *J. Phys. Chem.*, **80**, 8 (1976).—Chemically activated 1-buten-1-yl radicals were generated by the addition of ethyl radicals produced by the photolysis of diethylketone to acetylene at 75 and 123°. The unimolecular rate constant for the isomerization of the excited 1-buten-1-yl to 1-buten-4-yl radicals through 1,4-H atom migration was measured. In addition, it was found that the 1-buten-4-yl formed can isomerize to methylallyl radicals via 1,2-H atom shift. The average rate constants for isomerization were found to be 1.00×10^9 and $1.05 \times 10^9 \text{ sec}^{-1}$ for 1-buten-1-yl and 3.47×10^7 and $6.20 \times 10^7 \text{ sec}^{-1}$

for 1-buten-4-yl radicals at 75 and 123°, respectively. The best agreement between the rate constants as calculated by the RRKM theory and the experimental results was found when the threshold energies, E_0 , were chosen as 17.1 and 33.0 kcal/mol for 1,4- and 1,2-H atom shifts, respectively. It is shown that these values satisfy the expression, $E_0 = E_{ab} + E_s$, where E_{ab} is the activation energy for a bimolecular H atom abstraction and E_s is the ring strain energy.

Limits in the High Resolution Electron Microscopy of Halogen Substituted Organic Molecule Single Crystal Caused by Radiation Damage. T. Kobayashi and L. Reimer. *Bull. Inst. Chem. Res., Kyoto Univ.*, **53**, 105 (1975).—The decrease of the reflection intensities in electron diffraction diagrams of tetrabromoquinone, hexabromobenzene and hexadecachloro-copper-phthalocyanine single crystal films was used to obtain a quantitative measure of radiation damage. The films were obtained by epitaxial growth on KCl and NaCl cleavage planes. Two different methods were used for recording the integral reflection spot intensity. The first records the intensity of a diffraction diagram directly by a scanning method. The second employs photometry of a photographic plate with a rectangular spread of the spot, produced by a small scanning amplitude during the exposure. The electron diffraction spots disappear at charge densities (end point doses) in the specimen plane of 15–40 C.cm⁻² for hexadecachloro-copper-phthalocyanine, 2.0–2.9 C.cm⁻² for hexabromobenzene and 0.19–0.20 C.cm⁻² for tetrabromoquinone. The consequences for the imaging of lattice structures are discussed. There are differences in the damage dose for different reflections. The displacement u^{-2} are calculated by a Debye-Waller factor, but this value varies strongly for different reflections and decreases with increasing reciprocal lattice vector g , whereas for pure statistical displacements of the atoms there should be no dependence on g .

Formation and Properties of Various Amine Complexes of Iron- Phthalocyanine. T. Kobayashi, F. Kurokawa, and N. Uyeda. *Bull. Inst. Chem. Res., Kyoto Univ.*, **53**, 186 (1975).—The formation of additive complexes was studied in regard to iron-phthalocyanine (FePc) dispersed in various amines. The compositions were determined by means of weight-loss measurement and from the thermal behavior of the additive complexes as observed by DTA and X-ray powder diffraction. The decomposition temperature ranges from 100 to 300°C, above which the crystallites are converted into the β -form of pure FePc. Infrared absorption spectra indicated that amine molecules are coordinated to the central metal of FePc, while some extra molecules are freely included in the space of crystal lattice. From kinetic study of visible light absorption spectra, it was found that new absorption appears when the second molecule of the two is combined to the Fe atom of Pc-ring, indicating that a charge transfer mechanism is involved in the complex formation.

Effect of Through-Focusing on the Bright and Dark Field Molecular Images in High Resolution Electron Microscopy. K. Ishizuka and N. Uyeda. *Bull. Inst. Chem. Res., Kyoto Univ.*, **53**, 200 (1975).—The anticipated effect of through-focusing on the molecular images was investigated with the computer simulated high

resolution electron micrographs of the thin crystal of chlorinated-Cu-phthalocyanine. It was demonstrated that the molecular image reflecting the specimen structure will appear only at one focus position of through-focusing in the bright field mode for 500 kV electrons with the spherical aberration coefficient C_s of 1.0 and 1.8 mm. While in the dark field mode, only the heavy atoms in the molecule could be detected at the best focus position of through-focusing. For 100 kV electrons (with $C_s = 1.4$ mm), the simulated images did not resolve the molecular details in both the bright and the dark field modes, but the bright field mode was superior to the dark field one in a sense that the general molecular shape could be recognized at the best focus.

Dynamic Properties of Powder and Particle Characteristics. M. Arakawa and M. Nishino. *Bull. Inst. Chem. Res., Kyoto Univ.*, **53**, 256 (1975).—The diffusion process of powder particles into the vibrating powder bed was observed and the relation between the interparticle force and the dispersion property was investigated. The diffusion process of fine powder to the coarse powder bed is affected by not only the ratio of particle size, but also the particle-particle interaction force. For the interparticle force, the effect of the condensed film of water on the particle surface may be considered to be most important. In order to investigate the effects of these factors, the percolation properties through the beds of coarse powders of glass beads and of bronze spheres were examined by using surface treated fine glass beads as percolating powders. For the glass beads, it may be concluded that the phenomenon of segregation occurs with the difference of the surface property between particles.

Study of Microstructure of Mica and Montmorillonite by High Resolution Electron Microscopy. T. Yoshida. *Clay Science*, **5**, 1 (1976).—Clay minerals obtained from the weathering product of Ohya-ishi were examined by high resolution electron microscopy and selected area electron diffraction. Some mica crystals showed a unique morphology. They were very thin along the b -axis compared with c -axis. A high resolution electron micrograph showed a microstructure reflecting the arrangement of the tetrahedra in the unit layers of mica. Montmorillonite flakes showed a crossed lattice image of 4.5 Å spacing. A local ordering of unit layers in montmorillonite flakes was discussed.

Particle Size Measurement. M. Arakawa. *Chemistry (Kagaku)*, **30**, 28 (1975), in Japanese.—Review.

Electron Microscopy of Clay Minerals; Numbers of Stacking Layers Composing Organo-Montmorillonite Flake. T. Yoshida and E. Suito. *Sudo Toshio Kyoju Taikan Kinen Ronbunshu (Commemoration Issue dedic. to Prof. T. Sudo on his Retirement)*, 173 (1975), in Japanese.—Layer structures of the organo-montmorillonite flakes were observed by electron microscope. Frequency distribution curve of the numbers of stacking layers showed the maximum at 7 layers, and the results showed 13 layers per flake on the average. Curled shapes of the organo-montmorillonite flakes was discussed.

Solid-Liquid Adhesion of Oxidized Polyethylene Films: Effect of Temperature. A. Baszkin, M. Nishino, and L. Ter Minassian-Saraga. *J. Colloid and Interface Sci.*, **54**, 317 (1976).—The temperature effect on the wettability of oxidized polyethylene films with known surface densities shows a decrease in the free energy of adhesion at about 85°C for different liquids employed with varying numbers of OH groups. The thermograms obtained by differential thermal analysis show that the beginning of the melting transition is at about 85°C. The close agreement between the temperature at the beginning of the melting transition and decrease of the wettability of oxidized polyethylene films is interpreted by the increase of the chain mobility leading to the redistribution of external polar groups initially located at the solid-air interface. We express the observed phenomenon as a degree of the overturn of macromolecular chains. The results obtained are discussed in relation to the number of OH groups present in the liquids and their ability to form hydrogen bonds.

Molecular Image Reconstruction in High Resolution Electron Microscopy. N. Uyeda and K. Ishizuka. *J. Electron Microscopy*, **24**, 65 (1975).—A method to reconstruct a correct image reflecting the molecular structure of specimen has been devised in view of avoiding the drawback that electron micrographs, especially bright field ones, undergo striking changes in appearance with variation of defocusing. This method is available even for a single electron micrograph taken at an arbitrary defocus value. Computer simulations of this procedure demonstrated that the correct image clearly reflects the molecular structure and that the defocus value at which the original micrograph was taken is unequivocally determined.

Direct Observation of the Interstratified Structures in the Clay Minerals by Electron Microscopy. T. Yoshida. *J. Geo. Soc. Japan*, **12**, 354 (1976), in Japanese.—Layer structures of mixed layer clay minerals were examined by the mean of high resolution electron microscopy. Some of two dimensional lattice images observed in the a-b plane of mica/smectite mineral shows the displacement of b/4 of some layers. Lateral disorder of mixed layer structures was discussed.

The Effects of Mechanical Treatment of Kaolinite and Talc upon the Reinforcement of Rubber. T. Nukui, K. Kaida, Y. Furusawa, M. Arakawa, and E. Suito. *J. Soc. Rubber Ind., Japan*, **49**, 230 (1976), in Japanese.—The properties of the dry ground clays and the SBR compounded with them were examined. It was shown that the changes in particle surface properties as well as the changes in specific surface area by grinding were related to the physical properties of rubber.

The immersion heat had a good correlation with the rubber properties. Mooney viscosity was related to the immersion heat in water, and scorch time was related to the immersion heat in ethyl benzene. Tensile strength increased with the specific surface area of filler; there was a maximum at which the tensile strength began to decrease abruptly as the specific surface area increased. In the rubber compounded with high ground clay, the filler particles were not well dispersed and could be found as agglomerate. It seems that a decrease of tensile strength of the rubber compounded with the high ground clay causes the difficulty of dispersion of filler.

Computation of Electron Microscopical Images of Single Organic Molecules. T. Kobayashi and L. Reimer. *Optik*, **43**, 237 (1975).—It is useful for the imaging of the structure of single organic molecules to simulate the imaging parameters on a computer and to look for optimum imaging conditions. The contrast transfer functions of the objective lens and the calculated image intensity distributions of single atoms can alone give no information about the superposition and possible interference of the amplitude contributions of the single atoms in the molecule. We selected Br substituted Cu-phthalocyanine as a model molecule, since it offers the best conditions for imaging, because of its high radiation resistance. The influence of the spherical aberration constant, defocusing and the electron energy are discussed, together with the contrast transfer functions and the images of single Br atoms in the bright and dark field mode of a transmission electron microscope. As expected, decreasing spherical aberration and increasing electron energy result in a better resolution. For example, the following typical interference effect is obtainable. Under certain conditions, the Br atoms are resolved but the central Cu atom causes no decrease of intensity in the bright field mode because of interfering amplitude contributions by the neighboring atoms. A calculation using the optical reconstruction method of Marechal and Hahn at 100 keV, $C_s=2$ mm shows the same resolution as a image with $C_s=0.5$ mm in Scherzer focus.

Conductive Phthalocyanines under Very High Pressure. A. Onodera, N. Kawai, and T. Kobayashi. *Solid State Communications*, **17**, 775 (1975).—Vanadyl, thorium, lead, copper, zinc, and metal-free phthalocyanines become appreciably conductive under the static pressure of up to several hundred kilobars. The least resistivity observed is $0.1 \Omega\text{-cm}$ for vanadyl phthalocyanine. There appear minima in the curves showing resistance change with pressure for vanadyl, thorium, lead, and metal-free phthalocyanines.

Inorganic Chemistry

Conditions for the Formation of Compounds Consisting of BaO and Fe_2O_3 from Aqueous Suspensions. M. Kiyama. *Bull. Chem. Soc. Japan*, **49**, 1855 (1976).—Suspensions containing either iron (III) hydroxide or hydroxide oxide and barium ions were subjected to autoclaving at various temperatures from 100 to 300°C , and the properties of the resulting products were studied. A ferromagnetic precipitate, $\text{BaO}\cdot 6\text{Fe}_2\text{O}_3$, consisting of hexagonal plate-like particles, was obtained by suitable combination of temperature, kind, and particle size of iron (III) hydroxide oxide, and concentration of $\text{Ba}(\text{OH})_2$. Nonferromagnetic precipitates, $\text{BaO}\cdot 4.5\text{Fe}_2\text{O}_3$ and $\text{BaO}\cdot 2\text{Fe}_2\text{O}_3$, were also formed depending on the conditions. The mechanism of their formation is discussed. The magnetic properties of the $\text{BaO}\cdot 6\text{Fe}_2\text{O}_3$ precipitates are investigated.

Formation and Solubility of Basic Lead Chlorides at Different pH Values. M. Kiyama, K. Murakami, T. Takada, I. Sugano, and T. Tsuji. *Chem. Letters*, 23 (1976).—Suspensions prepared by mixing solutions of NaOH and PbCl_2 in various

mol ratios were subjected to aging at 25, 50, and 80°C. Formation of three kinds of basic lead chlorides takes place, depending mainly on the pH. Their solubilities in the suspension media with various pH values at 25°C were determined.

Chemistry of Iron (II) and (III) Hydroxides. M. Kiyama. *Funtai Oyobi Funmatsu-yakin (J. Japan. Soc. Powd. Metall.)*, **23**, 77 (1976), in Japanese.—Precipitates of Iron (II) and (III) hydroxides are formed, when alkaline solutions are added to iron salt solutions. By hydrolysis or oxidation, the precipitates are transformed into iron oxides (α -, γ -Fe₂O₃, and Fe₃O₄), hydroxide oxides (α -, β -, γ -, and δ -FeO(OH)), and basic salts depending on the conditions. In this paper, the conditions and the mechanism are reviewed for the transformation into each compound.

Mössbauer Spectroscopy in Ferromagnetic Metal Surface. T. Shinjo. *IEEE Trans. Mag.*, **Mag-12**, 86 (1976).—Mössbauer experiments were made utilizing Co⁵⁷ or Fe⁵⁷ as a microprobe for studying the magnetic properties of ferromagnetic metal surfaces. For the emission spectroscopy, carrier-free Fe⁵⁷ atoms were electrodeposited on a surface of bulk iron. The absorption spectroscopy was applied to a sample whose surface was selectively enriched with Fe⁵⁷. In both cases, the spectra at 4.2 K showed that all iron atoms in the surface are ferromagnetic, but the reduced hyperfine field suggests a partial decrease of the local magnetic moment.

Mössbauer Study of Supertransferred Hyperfine Field of ¹¹⁹Sn (Sn⁴⁺) in Ca_{1-x}Sr_xMnO₃. M. Takano, Y. Takeda, M. Shimada, T. Matsuzawa, T. Shinjo, and T. Takada. *J. Phys. Soc. Japan*, **39**, 656 (1975).—Ca_{1-x}Sr_xMn_{0.99}Sn_{0.01}O₃ (0 ≤ x ≤ 1) with (nearly) cubic perovskite structures were prepared and the magnetic hyperfine fields of ¹¹⁹Sn (Sn⁴⁺) were measured by the Mössbauer effect. The hyperfine fields arise from unpaired *s* electron spin densities transferred from Mn⁴⁺ ions (supertransferred hyperfine interaction). The hyperfine field for a tin ion was found to depend linearly upon the numbers of Ca²⁺ and Sr²⁺ ions in the neighboring divalent cation sites, with proportional coefficients having opposite signs. To explain experimental results two kinds of spin transfer processes contributing to the hyperfine field oppositely to each other have been considered, and spin transfer via a divalent cation is emphasized particularly. The hyperfine field at 0 K for Sn⁴⁺ in CaMnO₃ is -75 kOe, while +20 kOe for Sn⁴⁺ in SrMnO₃.

Magnetic Susceptibility and Torque Measurements of FeV₂S₄, FeV₂Se₄, and FeTi₂Se₄. S. Muranaka and T. Takada. *J. Solid State Chem.*, **14**, 291 (1975).—Magnetic susceptibility and torque measurements of FeV₂S₄, FeV₂Se₄, and FeTi₂Se₄ were made using the powder and the single crystal samples. The inverse susceptibility of FeV₂S₄, FeV₂Se₄, and FeTi₂Se₄ changed its slope at 850, 820, and 700 K, respectively, at which temperature the order-disorder transition of cation vacancies should seem to take place. Above these temperatures the paramagnetic moment obtained for these compounds was in the range of 5.26–5.37 μ_B , close to that of the high spin state Fe²⁺. Below these temperatures the paramagnetic moment was reduced to 4.2y–4.35 μ_B .

The antiferromagnetic spin axis of FeV_2S_4 was in the neighborhood of the [101] direction and that of FeV_2Se_4 and FeTi_2Se_4 in the direction of the c -axis. The large magnetic anisotropy observed and the preference of the magnetic moments for the direction of the c -axis were attributed to the spin-orbit interaction of Fe^{2+} electrons in the trigonal crystal field.

The Magnetic Properties of Ultrafine Particles of $\text{Ni}(\text{OH})_2$. H. Miyamoto. *Mat. Res. Bull.*, **11**, 599 (1976).—Ultrafine particles of $\text{Ni}(\text{OH})_2$ were prepared by precipitation from aqueous solution. The susceptibility of the ultrafine particles shows a distinctive maximum at temperature which is rather lower than T_N of the large particles. Using the c -axis oriented ultrafine particles prepared by the sedimentation method, the magnetic susceptibility and the magnetization curve perpendicular and parallel to the c -axis of the ultrafine particles were measured. The magnetization curve showed a small hysteresis in low field and a remanent magnetization which increased with decrease of the particle size. Two-step jump was observed in the magnetization curve of the ultrafine particles when the external field was applied along the c -axis. The magnetic properties characteristic of the $\text{Ni}(\text{OH})_2$ ultrafine particles are discussed.

Removal of Heavy Metal Ions from Waste Water by Ferritization. T. Takada. *Sekiyu-Gakkaishi (J. Japan Petro. Inst.)*, **19**, 275 (1976), in Japanese.—The technique for the ferrite formation is useful to remove heavy metal ions from waste water.

The properties of spinel ferrite, the principle of the chemical reaction and the results of practical test are described.

Epitaxial Nucleation. Y. Bando. *Kagaku Sosetsu*, No. 9, 73 (1975), in Japanese.—Some theories on epitaxial nucleation were reviewed and studies on oxidation of metals and precipitation from aqueous solution were presented.

Chemical Transport Reaction (1). Y. Bando. *Kagaku Sosetsu*, No. 9, 136 (1975), in Japanese.—Physical chemistry in chemical transport reaction and its application to solid state chemistry were reviewed.

Application of Mass Spectrometer to Ceramic Material Research. Y. Bando. *Seramikkusu (Ceramics)*, **11**, 65 (1976), in Japanese.—Application of quadrupole mass spectrometer to researches of reactive evaporation, high temperature reaction using Kundsen cell, solid-gas reaction and chemical transport reaction were reviewed.

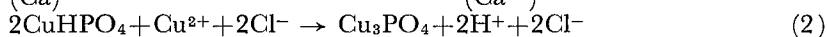
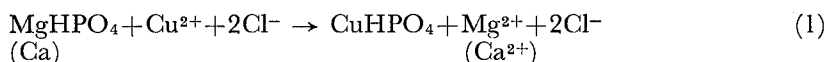
Oriented Polycrystalline Oxide Ceramics Fabricated by Unidirectional Solidification of Their Melts. M. Tashiro, T. Kokubo, S. Ito, and M. Arioka. *Bull. Inst. Chem. Res., Kyoto Univ.*, **53**, 471 (1975).—The ceramics consisting of unidirectionally oriented crystals can be fabricated by unidirectional solidification of the oxide melts. They exhibit special features in a specific direction. The state of knowledge and understanding of the process of unidirection solidification of the oxide

melts, the microstructure of the resultant polycrystalline oxide ceramics, and their physical properties are reviewed. The results of investigation on the above subjects recently carried out in the authors' laboratory are incorporated in the present review.

Crystallized Glass. M. Tashiro. *Kotai Butsuri*, **11**, 163 (1976), in Japanese.—Crystallization process of glasses, and properties and applications of crystallized glasses are reviewed in Japanese.

Adsorptive Properties of Cu (II) on $\text{CaHPO}_4 \cdot 2\text{H}_2\text{O}$ and $\text{MgHPO}_4 \cdot 3\text{H}_2\text{O}$ Powders in Aqueous Solutions. T. Maki and M. Ohkubo. *Nippon Kagaku Kaishi* (*J. Chem. Soc. Japan, Chem. Ind. Chem.*), **50** (1976), in Japanese.—Powders of commercially available calcium hydrogenphosphate dihydrate ($\text{CaHPO}_4 \cdot 2\text{H}_2\text{O}$) or magnesium hydrogenphosphate trihydrate ($\text{MgHPO}_4 \cdot 3\text{H}_2\text{O}$) (composed of particles ranging 1–100 μ in diameter) were immersed in copper (II) sulfate or copper (II) chloride solutions containing 100–2500 ppm of Cu (II) for 0–48 hrs at room temperature and adsorption ability and mechanism of Cu (II) were investigated by measuring amounts of Cu (II), Ca (II) or Mg (II) and P (V) in the residual solutions and by analysing x-ray diffraction patterns of the powders before and after adsorption. The results were as follows:

- 1) Although the powders dissolved a little into solution, the adsorption progressed with processes, in which the powders changed to Cu (II)-containing insoluble phosphates in the solution of pH range 3.0–7.0.
- 2) When they were immersed in the solutions containing 1500 or 2500 ppm of Cu (II), their uptakes of Cu (II) were fairly larger than those of other phosphates and commercial adsorbents, and their values both amounted to about 7.0 meq Cu/g.
- 3) The adsorption mechanism of the powders immersed into the copper (II) chloride solutions was explained with following formulas.



when there were excess Cu (II) in the solution, $\text{CuHPO}_4 \cdot \text{H}_2\text{O}$ produced by reaction (1) is instantaneously converted to $\text{Cu}_3(\text{PO}_4)_2 \cdot 3\text{H}_2\text{O}$ by capturing excess Cu (II) by reaction (2). However, when the amounts of Cu (II) in the solutions decrease until a certain value by adsorption, only the reaction (1) proceeds again as in the solutions of low Cu (II) concentrations.

Organic Chemistry

Mechanism of Benzyl Migration from Nitrogen to Carbon in Enamines. J. Oda, T. Igarashi, and Y. Inouye. *Bull. Inst. Chem. Res., Kyoto Univ.*, **54**, 119 (1976).—The rearrangement of (*R*)-*N*-isobutenyl-*N*-methyl-benzylamine-*a-d* was thermally effected to give (*R*)-2,2-dimethyl-3-phenyl-propanal-3-*d* with over-all retention of configuration of the migrating terminus in 91% asymmetric yield. The stereochemical outcome in the present benzyl migration unequivocally established the mechanism to

be the sequential *N*-alkylation, retrogressive dissociation, and *C*-alkylation, with two Walden inversions involved in the process.

Asymmetric [3,3]Sigmatropic Rearrangement of Allylic Enamine. J. Oda, T. Igarashi, and Y. Inouye. *Bull. Inst. Chem. Res., Kyoto Univ.*, **54**, 180 (1976).—(*R*)-(+)-*N*-Methylphenylethylamino-*E*-propene, when heated with allyl bromide in acetonitrile, followed by hydrolysis, gave 2-methyl-4-pentenal, which was converted by silver oxide oxidation into (+)-2-methyl-4-pentenoic acid of the well-defined *S*-configuration. The stereochemistry of the present chiral system, involving a [3,3] sigmatropic rearrangement of the first formed ammonium salt, was interpreted in terms of the possible diastereomeric transition state conformations, in the light of the Woodward-Hoffmann rule.

Asymmetric Amination I. Asymmetric Synthesis of Aspartic Acid and Evaluation of Optical Yield in the Addition Reaction of Chiral Phenethylamine to α,β -Unsaturated Esters. Y. Nakajima, J. Oda, and Y. Inouye. *Agr. Biol. Chem.*, **39**, 2065 (1975).—The enantioselective addition of chiral benzylic amines to dimethyl maleate and fumarate gives optically active aspartic acid in satisfactory yields. The *re*-face favorably meets the stereochemical requirements of the chiral *R*-amines than does the *si*-face. The stereoselectivity in the present reaction is little dependent on solvent polarity but is significantly enhanced by low temperature. The direct determination by vpc of the diastereomeric products provides more precise values of optical yield and is preferred to the polarimetry of the end product after many steps of transformation with probable fractionations.

Application of Dibenzoate Chirality Rule to Flexible Systems. Y. Yamamoto, M. Fushimi, J. Oda, and Y. Inouye. *Agr. Biol. Chem.*, **39**, 2223 (1975).—The chiroptical properties of (+)-(1*S*,2*S*)-dibenzooxycyclooctane were observed. The dibenzoate rule for chiral dibenzooxycyclohexanes was successfully applicable to these medium-sized ring compounds as well. The conformation of the open chain dibenzoate was discussed on the basis of chiroptical properties found for the dibenzoate and di-*p*-nitrobenzoate of (2*S*,3*S*)-butane-diol.

An NAD(P)H Model Reaction: Reduction of α -Ketoesters by the Hantzsch Ester Accelerated by Zinc Complex in the Reformatsky Mixture. K. Nishiyama, N. Baba, J. Oda, and Y. Inouye. *Agr. Biol. Chem.*, **40**, 821 (1976).—The hydrogen transfer from the Hantzsch ester to pyruvate and benzoylformate was achieved by the catalysis of a mono-ionized zinc species formed in the Reformatsky reaction.

Reaction of Quinolinium Salts with 1,4-Dihydronicotinamides. N. Baba, K. Nishiyama, J. Oda, and Y. Inouye. *Agr. Biol. Chem.*, **40**, 1259 (1976).—*N*-Alkyl-1,4-dihydronicotinamide easily underwent oxidation by *N*-carboalkoxyquinolinium bromide in nearly quantitative yields. This provides by far the simpler and convenient method for preparation of 1,4-dideuteriated nicotinamide derivatives in satisfactory yields.

Self-Immolative Asymmetric Synthesis. I. Allylic Rearrangement of Optically Active Amine Oxide. M. Moriwaki, Y. Yamamoto, J. Oda, and Y. Inouye. *J. Org. Chem.*, **41**, 300 (1976).—Transfer of chirality from tetracoordinate nitrogen to trigonal carbon was achieved in the allylic rearrangement of (*R*)-(+)-*N*-*trans*-crotyl-*N*-methyl-*p*-toluidine oxide to (*S*)-(+)-*O*-methylvinylcarbiny-*p*-tolylhydroxylamine with nearly complete conservation of chirality. The present thermally allowed [2,3]sigmatropic rearrangement proceeds via a transition state conformation such as to meet the orbital symmetry requirements in a doubly suprafacial fashion.

Self-Immolative Asymmetric Synthesis. II. Transfer of Chirality from Tetrahedral Carbon to Trigonal Carbon in Chiral Amine Oxide Rearrangement. Y. Yamamoto, J. Oda, and Y. Inouye. *J. Org. Chem.*, **41**, 303 (1976).—The [2,3]sigmatropic rearrangement of (*S*)-*N,N*-dimethyl-3-(*trans*-1-phenyl-1-butenyl)-amine oxide to give (*S*)-*O*-*trans*-1-phenyl-2-butenyl-*N,N*-dimethylhydroxylamine was effected at -20°C with nearly complete transfer of chirality from tetrahedral carbon to trigonal carbon. At higher temperature, the radical path prevailed to yield exclusively the [1,2] shift product, *O*-*trans*-1-methyl-3-phenyl-2-propenyl-*N,N*-dimethylhydroxylamine, with conservation of chirality to the extent of 20%.

Absolute Configuration of 3-Amino-1-phenylbutane. Y. Yamamoto, J. Oda, and Y. Inouye. *Bull. Chem. Soc. Japan*, **48**, 3744 (1975).—The absolute configuration of (–)-3-amino-1-phenylbutane was established by the correlation to (*R*)-(–)-*N*-benzoylalanine methylester via (+)-*trans*-3-amino-1-phenylbut-1-ene.

Asymmetric Reduction of α -Ketoesters with Hantzsch Esters (Dialkoxycarbonyldihydropyridines). K. Nishiyama, N. Baba, J. Oda, and Y. Inouye. *J.C.S. Chem. Commun.*, 104 (1976).—Single and double asymmetric inductions were achieved by the reduction of pyruvates and benzoylformates with 2,6-dimethyl-3,5-dialkoxycarbonyl-1,4-dihydropyridine in the presence of a mono-ionized zinc species; differentiation is made between enantiotopic faces of the substrate carbonyl by homotopic hydrogen, and between diastereotopic faces by equivalent and diastereotopic hydrogen.

Terpenoids-XXXIV. Teucvidin, a Minor Norditerpene from *Teucrium viscidum* var. *Miquelianum*. I. Uchida, T. Fujita, and E. Fujita. *Tetrahedron*, **31**, 841 (1975).—The structure and stereochemistry of teucvidin, a novel minor norditerpene isolated from *Teucrium viscidum* var. *Miquelianum*, was determined on the basis of spectroscopic evidence and X-ray analysis. The INDOR spectroscopy proved very useful and its application was discussed in detail in this paper.

Confirmation of the Structure of Calliterpenone, a Diterpene from *Callicarpa macrophylla* (Terpenoids-XXXV). E. Fujita, M. Ochiai, I. Uchida, A. Chatterjee, and S. K. Desmukh. *Phytochemistry*, **14**, 2249 (1975).—The structure and absolute configuration of calliterpenone was established as 3-oxo-13 β -kaurane-16 α ,17-diol. This conclusion confirms that proposed by Ahmad and Zaman, and the formula suggested previously by Chatterjee *et al.* is revised.

Syntheses of Methyl Esters of Gibberellin A₁₅ and Gibberellin A₃₇. M. Node, H. Hori and E. Fujita. *J. C. S. Chem. Comm.*, 898 (1975).—The total synthesis of gibberellin A₁₅ methyl ester and gibberellin A₃₇ methyl ester from 5-methoxy-2-tetralone *via* a key intermediate was accomplished. The key compound was easily derived from enmein and used as a relay. Thus, the chemical conversion of enmein into the foregoing gibberellin methyl esters was also achieved.

Reactions of *ent*-16- and *ent*-15-Kaurenes with Thallium (III) Trinitrate and a Sigmatropic Rearrangement between the Allylic Nitrate Products. M. Ochiai and E. Fujita. *J. C. S. Chem. Comm.*, 967 (1975).—The reactions of both *ent*-16-kaurene and *ent*-15-kaurene with thallium (III) trinitrate resulted in the formation of the allylic nitrates. A [3,3]-sigmatropic rearrangement between these allylic nitrates was observed, when each nitrate was heated in benzene in a sealed tube at 100°C for 25 hours.

The Chemistry on Diterpenoids in 1973. E. Fujita, K. Fuji, Y. Nagao, and M. Node. *Bull. Inst. Chem. Res., Kyoto Univ.*, **53**, 319 (1975).—This is one of our annual review series on diterpenoids. It quotes 241 references.

The Chemistry on Diterpenoids in 1974. E. Fujita, K. Fuji, Y. Nagao, M. Node, and M. Ochiai. *Bull. Inst. Chem. Res., Kyoto Univ.*, **53**, 494 (1975).—This is also one of our annual review series on diterpenoids. It quotes 227 references.

A New Carbon-Carbon Bond Formation at the β -Position of 3,4-Dimethoxy-*E*- β -nitrostyrene. Y. Nagao, K. Kaneko, and E. Fujita. *Tetrahedron Lett.*, 1215 (1976).—A new method for a carbon-carbon bond formation at the β -position of 3,4-dimethoxy-*E*- β -nitrostyrene was developed. Thus, a selective synthesis of a sole geometric *E*-isomer of 3,4-dimethoxy- β -substituted- β -nitrostyrene was accomplished starting from 3,4-dimethoxy-*E*- β -nitrostyrene *via* a Michael-type reaction with α -(3,4-dimethoxyphenyl)- β -nitroethylthioethane derived from the starting material by addition of ethane thiol and subsequent stereoselective elimination.

A New Transformation of Thioethers into Ethers Using Thallium (III) Nitrate. Y. Nagao, K. Kaneko, M. Ochiai, and E. Fujita. *J. C. S. Chem. Comm.*, 202 (1976).— α -(3,4-Dimethoxyphenyl)- β -nitroethylthioethane on treatment with 1.2 mol. equiv. of thallium (III) trinitrate in several alcohols at room temperature afforded α -(3,4-dimethoxyphenyl)- β -nitroethoxyalkanes in good yield. Thus, a new transformation of thioethers into ethers was developed.

Dethioacetalization with Thallium (III) Nitrate. E. Fujita, Y. Nagao, and K. Kaneko. *Chem. Pharm. Bull.*, **24**, 1115 (1976).—Several thioacetals were dethioacetalized by their treatment with thallium (III) nitrate under mild conditions for a short time to recover the parent carbonyl compounds in good yields.

This novel method will promise the increasing value of the ethylenedithioacetal function for the protection of the carbonyl group especially in the field of the syntheses of the complex natural products.

Antitumor Activity of the *Isodon* Diterpenoids: Structural Requirements for the Activity. E. Fujita, Y. Nagao, M. Node, K. Kaneko, S. Nakazawa, and H. Kuroda. *Experientia*, **32**, 203 (1976).—A significant antitumor activity of oridonin and lasiokaurin, the kaurene-type diterpenoids of *Isodon* species, was shown by their i.p. injection to the test mice inoculated by Ehrlich ascites carcinoma. Enmein, 14R-hydroxyisodocarpin, and 14-deoxyoridonin were also active under larger dose. The relationship between their chemical structure and antitumor activity was investigated, and the activity of oridonin and lasiokaurin was rationalized in terms of their structural feature.

The Chemistry on Diterpenoids in 1975. Part I. E. Fujita, K. Fuji, Y. Nagao, M. Node, and M. Ochiai. *Bull. Inst. Chem. Res., Kyoto Univ.*, **54**, 197 (1976).—This is also one of a series of our annual reviews on diterpenoids chemistry. This review covers the literature published between January and June 1975. It quotes 136 references.

Lythraceous Alkaloids. E. Fujita and K. Fuji. *International Review of Science, Series 2*, **9**, 119 (1976).—This is a review on the chemistry of the alkaloids of the Lythraceae plants. The Lythraceous alkaloids have been investigated mainly in Japan and U.S. This review quoting 72 references includes structure determination, synthesis, and biosynthesis of the Lythraceous alkaloids. The important sections of lythranine and lythrancine-lythrancepine groups are concerned with the authors' own works.

Total Synthesis of Indole and Dihydroindole Alkaloids. VIII. Studies on the Synthesis of Bisindole Alkaloids in the Vinblastine-Vincristine Series. The Chloroindolenine Approach. J. P. Kutney, J. Beck, F. Bylsma, J. Cook, W. J. Cretney, K. Fuji, R. Inhof, and A. M. Treasurywala. *Helv. Chim. Acta.*, **58**, 1690 (1975).—As a part of the total synthesis of dimeric indole alkaloids, vinblastine and vincristine, which are regarded as important clinical agents for the treatment of various cancers in humans, studies on the synthesis of 18'-epi-4'-deoxo-4'-epivinblastine and related analogues are described in this paper.

Palladium-Catalyzed Decomposition of Azide. Formation of Benzonitrile from Benzyl Azide. H. Hayashi, A. Ohno, and S. Oka. *Bull. Inst. Chem. Res., Kyoto Univ.*, **53**, 489 (1975).—Palladium metal catalyzes the decomposition of benzyl azide affording benzonitrile, benzylamine, and benzyldiene-benzylamine. The presence of a suitable hydrogen-acceptor improves the yield of benzonitrile at the sacrifice of benzylamine, whereas the yield of benzyldienebenzylamine remains constant. A plausible scheme has been proposed for the reaction.

Nitration of 9-Ethyl-10-methylanthracene, 9-Ethylanthracene, and 9-Methylanthracene. H. Suzuki, H. Yoneda, T. Hanafusa, and T. Sugiyama. *Bull. Inst. Chem. Res., Kyoto Univ.*, **54**, 176 (1976).—9,10-Dimethylanthracene and 9,10-diethylanthracene behave quite differently towards the action of nitric acid; the

former compound has been shown to undergo side-chain nitration to give a nitro-methyl derivative, while the latter gives rise to an addition product. In order to confirm the strikingly different behavior of the methyl group as compared to the ethyl group towards nitrating agent, we have extended the investigation to include three additional 9-alkylanthracenes.

Di-*tert*-butyl Thioketone. A. Ohno, K. Nakamura, Y. Nakazima, and S. Oka. *Bull. Chem. Soc. Japan*, **48**, 2403 (1975).—Di-*tert*-butyl thioketone, a new aliphatic thioketone, has been prepared from sodium salt of di-*tert*-butyl ketimine and carbon disulfide, and its IR and UV spectral properties are studied.

Nucleophilic Displacement Catalyzed by Transition Metal. I. General Consideration of the Cyanation of Aryl Halides Catalyzed by Palladium (II). K. Takagi, T. Okamoto, Y. Sakakibara, A. Ohno, S. Oka, and N. Hayama. *Bull. Chem. Soc. Japan*, **48**, 3298 (1975).—The displacement reaction of various non-activated aryl halides with cyanide ions was investigated in the presence of palladium salts. Various aryl iodides and bromides were converted into the corresponding aryl cyanides in good yields under mild conditions. The addition of certain substances, such as potassium hydroxide and potassium carbonate, enhanced the catalytic activity. Hexamethylphosphoric triamide, in which potassium cyanide was scarcely soluble, was an outstanding solvent for the reaction. The reduced palladium species was supposed to be the active catalyst.

Charge-Transfer Intermediate in the Reaction of Thioketone with Nucleophiles. A. Ohno, K. Nakamura, M. Uohama, S. Oka, T. Yamabe, and S. Nagata. *Bull. Chem. Soc. Japan*, **48**, 3718 (1975).—Thiobenzophenone reacts with butyllithium, phenyllithium, and sodium ethoxide in ethanol giving benzhydryl butyl sulfide, benzhydryl phenyl sulfide, and dibenzhydryl disulfide, respectively. On the other hand di-*tert*-butyl thioketone affords 2,2,4,4-tetramethylpentane-3-thiol, 2,2,4,4-tetramethyl-3-phenylpentane-3-thiol, and 2,2,4,4-tetramethylpentane-3-thiol by the reaction with butyllithium, phenyllithium, and sodium ethoxide in ethanol, respectively. Product analyses and tracer experiments with deuteriums have revealed that these reactions proceed through a charge-transfer mechanism.

Palladium-Catalyzed Decomposition of Azides. I. Formation of Nitriles. H. Hayashi, A. Ohno, and S. Oka. *Bull. Chem. Soc. Japan*, **49**, 506 (1976).—Palladium metal catalyzes the decomposition of benzyl azide affording benzonitrile, benzylamine, and *N*-benzylidene-benzylamine. The presence of a suitable hydrogen-acceptor improves the yield of benzonitrile at the sacrifice of benzylamine, whereas the yield of *N*-benzylidenebenzylamine remains constant. The reaction is applied to the preparation of other nitriles.

Palladium(O) Catalyzed Syntheses of Ketones from Acyl Halides and Organomercury (II) Compounds. K. Takagi, T. Okamoto, Y. Sakakibara, A. Ohno, S. Oka, and N. Hayama. *Chem. Lett.*, 951 (1975).—Convenient syntheses

of various ketones from acyl halides and organomercury (II) compounds have been achieved by the aid of catalytic amounts of tetrakis (triphenyl-phosphine) palladium in hexamethylphosphoric triamide. Plausible reaction path is proposed.

Reactions of Di-*tert*-butyl Thioketone. A. Ohno, K. Nakamura, M. Uohama, and S. Oka. *Chem. Lett.*, 983 (1975).—New type of reactions of di-*tert*-butyl thioketone with phenyllithium, alkyllithiums, sodium cyanide, hydrogen cyanide, sulfuric acid, and hydrogen peroxide are reported

NO₂ Catalyzed Chlorination of Anthracene by Metal Halides. T. Sugiyama, K. Tanioka, A. Ohno, and S. Oka. *Chem. Lett.*, 307 (1976).—In the presence of nitrogen dioxide, aluminum chloride and some other metal chlorides have been found to be highly selective and regiospecific chlorinating agents for anthracene.

Reduction by a Model of NAD(P)H. IX. ESR Study on the Biomimetic Reduction of Benzils with 1-Benzyl-1,4-dihydronicotinamide. Y. Ohnishi and A. Ohno. *Chem. Lett.*, 697 (1976).—ESR studies on the biomimetic reduction of benzils by 1-benzyl-1,4-dihydronicotinamide indicate the formation of anion radicals of benzils. In the presence of magnesium perchlorate, the anion radicals are found to coordinate onto the metal ions.

Reduction by a Model of NAD(P)H. VIII. Effects of Metal Ion on the Course and Stereochemistry of the Biomimetic Reduction of Olefin. Y. Ohnishi, M. Kagami, T. Numakunai, and A. Ohno. *Chem. Lett.*, 915 (1976).—Asymmetric reduction of an olefin is achieved with a chiral NAD(P)H-model compound in the presence of magnesium perchlorate which represses a side reaction catalyzed by a base.

Reduction by a Model of NAD(P)H. Effect of Metal Ion and Stereochemistry on the Reduction of α -Keto Esters by 1,4-Dihydronicotinamide Derivatives. Y. Ohnishi, M. Kagami, and A. Ohno. *J. Amer. Chem. Soc.*, **97**, 4766 (1975).—The first example for stereospecific biomimetic reduction of α -keto esters by derivatives of 1,4-dihydronicotinamide substituted by a chiral group at an amide-nitrogen is reported. It is also found that a divalent metal cation, but not a univalent cation, catalyzes the reduction. A plausible mechanism has been proposed.

Reduction by a Model of NAD(P)H. Reduction of α -Diketones and α -Keto Alcohols by 1-Benzyl-1,4-dihydronicotinamide. Y. Ohnishi, M. Kagami, and A. Ohno. *Tetrahedron Lett.*, 2437 (1975). Biomimetic reductions of α -diketones and α -keto alcohols by 1-benzyl-1,4-dihydronicotinamide, a model of NAD(P)H, are reported. In this model reaction, magnesium ion plays a role of alcohol dehydrogenase in enzymic reactions. It has also been found that the model reaction is accelerated with the irradiation with light.

Reduction by a Model of NAD(P)H. X. Asymmetric Reductions of Carbonyl Compounds in the Presence of Magnesium Perchlorate. Y.

Ohnishi, T. Numakunai, T. Kimura, and A. Ohno. *Tetrahedron Lett.*, 2699 (1976).—Optical yields of products from biomimetic asymmetric reductions of 2-acetylpyridine, 2-benzoylpyridine, and ethyl benzoylformate by a chiral N- α -methylbenzyl-*n*-propyl-1,4-dihydronicotinamide, a model of NAD(P)H, depend on the ratio of concentrations of magnesium ion and the model compound. For acylpyridines, the yields decrease with the increase of the ratio, $[Mg^{++}]/[Model]$, whereas it increases with the increase of the ratio for ethyl benzoylformate.

Reduction by a Model of NAD(P)H. Contribution of Metal Ion to Asymmetric Reduction of Trifluoroacetophenone. Y. Ohnishi, T. Numakunai, and A. Ohno. *Tetrahedron Lett.*, 3813 (1975).—Trifluoroacetophenone is reduced by N- α -methylbenzyl-1-*n*-propyl-1,4-dihydronicotinamide, a chiral model of NAD(P)H, in acetonitrile with or without magnesium ion. However, no asymmetric induction takes place without magnesium ion. Magnesium ion also accelerates the reduction. Thus, magnesium ion in the present biomimetic reduction exerts similar effect to that of alcohol dehydrogenases in enzymic reductions.

The Reaction of Alkyl Halides with Mercuric Thiocyanate in Tetrahydrofuran. The Solvent Incorporation and the Intermediacy of O-Alkyl-tetrahydrofuranium Ions. N. Watanabe, S. Uemura, and M. Okano. *Bull. Chem. Soc. Japan*, 48, 3205 (1975).—The reaction of alkyl halides with mercuric thiocyanate in tetrahydrofuran (THF) affords mainly the THF-incorporated products, $R[O(CH_2)_4]_nNCS$ and $R[O(CH_2)_4]_nSCN$ (mostly $n=1$ and 2), where the isomer ratios (N/S ratios) are nearly 1. The reaction of $EtO(CH_2)_mBr$ ($m=2-5$) with mercuric thiocyanate in THF or *n*-Bu₂O proceeds rapidly only in the case of $m=4$ to give $EtO(CH_2)_4NCS$ and $EtO(CH_2)_4SCN$, the N/S ratio being also nearly 1, and gives $EtNCS$ and $EtSCN$ when $m=5$, while the reaction with potassium thiocyanate in DMF affords a good yield of $EtO(CH_2)_mSCN$ ($m=2-5$) as nearly the only product. It is suggested that the titled reaction involves the initial formation of a five-membered oxonium ion, O-alkyltetrahydrofuranium ion, and a subsequent attack by $XHg(SCN)_2^-$.

Oxidation of Isocyanides by Hg (II), Tl (III), and Pb (IV) Acetates. S. Tanaka, H. Kido, S. Uemura, and M. Okano. *Bull. Chem. Soc. Japan*, 48, 3415 (1975).—Isocyanides were oxidized to isocyanates in acetic acid in the presence of Hg (II), Tl (III), or Pb (IV) acetate through acetoxymetallation. The reaction of an isocyanide with Tl (III) acetate in various alcohols gave the corresponding carbamates in good yields.

The Chlorination of Norbornene by Metal Chlorides and the Product Isomerization. S. Uemura, A. Onoe, and M. Okano. *Bull. Chem. Soc. Japan*, 48, 3702 (1975).—The reaction of norbornene with $CuCl_2$, $TiCl_3 \cdot 4H_2O$, $PbCl_4$, $SeCl_4$, $SbCl_5$, and VCl_4 in CCl_4 , CH_2Cl_2 , or CH_3CN gave a mixture of nortricyclyl chloride (1), and six isomeric dichloronorbornanes [*trans*-2,3-(2), *exo*-2-*anti*-7-(3), *trans*-2,5-(4), *exo*-*cis*-2,5-(5), *exo*-*cis*-2,3-(6), and *exo*-2-*syn*-7-(7)], the product distribution de-

pending very much on metal chlorides and reaction conditions. The reactions did not show any participation of a chlorine molecule which may be released from metal chlorides. The ability of SeCl_4 and VCl_4 to chlorinate olefins was found for the first time. From a synthetic viewpoint CuCl_2 was a good reagent for obtaining **2**, while $\text{TiCl}_3 \cdot 4\text{H}_2\text{O}$ and SbCl_5 were recommended for either **3** or **7**. The reactions with the following metal chlorides did not give any dichloronorbornanes; SnCl_4 , BiCl_3 , TiCl_4 , FeCl_3 , NbCl_5 , TaCl_5 , and WCl_6 . It was revealed that isomerization of **2** or **7** to a mixture of **3**, **4**, and **5** occurred very rapidly by SbCl_5 and smoothly by $\text{TiCl}_3 \cdot 4\text{H}_2\text{O}$. The chlorination of norbornene and their products isomerization were mainly explained by assuming a chloronorbornyl cation as an intermediate.

The Chlorination of Norbornadiene by Various Chlorinating Agents.

A. Onoe, S. Uemura, and M. Okano. *Bull. Chem. Soc. Japan*, **49**, 345 (1976).—The chlorination of norbornadiene by CuCl_2 , $\text{TiCl}_3 \cdot 4\text{H}_2\text{O}$, SbCl_5 , SeCl_4 , and VCl_4 in CCl_4 or CH_3CN afforded mainly *trans*-3,5-(**1**) and *exo-cis*-3,5-dichloronorbornene (**2**). In the reaction with PbCl_4 , Cl_2 , SO_2Cl_2 , and PCl_5 , appreciable amounts of *exo*-5-*syn*-7-(**3**) and/or *exo-cis*-5,6-dichloronorbornene (**4**) were obtained besides **1** and **2**.

The Chlorination of 1,3- and 1,5-Cyclooctadienes with Various Chlorinating Agents. S. Uemura, A. Onoe, H. Okazaki, M. Okano, and K. Ichikawa. *Bull. Chem. Soc. Japan*, **49**, 1437 (1976).—The chlorination of 1,3-cyclooctadiene with various chlorinating agents gave an isomeric mixture of *trans*-3,4-, *cis*-3,4-, *trans*-3,8-, and *cis*-3,8-dichlorocyclooctane. From 1,5-dicyclooctadiene an isomeric mixture of *trans*- and *cis*-5,6-dichlorocyclooctane was obtained. The isomer distribution depended a great deal on chlorinating agents in both cases.

The Reactions of Polychloroethanes with Phenolate and Benzenethiolate Ions in Dipolar Aprotic Solvents. S. Tanimoto, R. Taniyasu, T. Takahashi, T. Miyake, and M. Okano. *Bull. Chem. Soc. Japan*, **49**, 1931 (1976).—The reactions of several *gem*- and *vic*-polychloroethanes containing 3–5 Cl atoms with PhONa in dimethyl sulfoxide and with PhSNa in *N,N*-dimethylformamide were examined. Either the mono-, di-, or tetra-substituted compounds of polychloroethylenes were obtained as the main products, depending on the kinds of substrates as well as on the amounts of the bases. The reaction products from polychloroethylenes with 2–4 Cl atoms were also examined under similar conditions for the sake of comparison. Reasonable reaction paths leading to these products were given.

Z-Chlorination of Alkylphenylacetylenes with Antimony Pentachloride. S. Uemura, A. Onoe, and M. Okano. *J. Chem. Soc. Chem. Comm.*, 145 (1976).—Reaction of alkylphenylacetylene with SbCl_5 in carbon tetrachloride gives the corresponding dichloroalkenes in fair yields, Z-addition predominating.

Acetoxythallation of Terminal Acetylenes. S. Uemura, H. Miyoshi, H. Tara, M. Okano, and K. Ichikawa. *J. Chem. Soc. Chem. Comm.*, 218 (1976).—The

reaction of terminal acetylenes with $\text{TI}(\text{OAc})_3$ in chloroform gives a new type of oxythallation adduct; this was shown to be one of the intermediates in the thallium (III) salt-catalyzed conversion of terminal acetylenes into ketones.

Stereochemistry of Chlorination and Chloriodination of Alkylphenyl-acetylenes by CuCl_2 . S. Uemura, A. Onoe, and M. Okano. *J. Chem. Soc. Chem. Comm.*, 925 (1975).—Reaction of alkylphenylacetylenes, $\text{PhC}\equiv\text{CR}$ ($\text{R}=\text{H}$ or alkyl) (**1**), with $\text{CuCl}_2\text{-LiCl}$ or $\text{CuCl}_2\text{-I}_2$ in acetonitrile gives the corresponding dihalogeno-alkenes in good yields; E-addition is favored except in the chlorination of (**1**, $\text{R}=\text{Bu}'$) where Z-addition predominates.

Reactions of 4-Chlorothiopyrylium Cation with Nucleophiles. S. Yoneda, T. Sugimoto, O. Tanaka, Y. Moriya, and Z. Yoshida. *Tetrahedron*, **31**, 2669 (1975).—Reactions of 4-chlorothiopyrylium cation (**1**) with a variety of nucleophiles have been investigated. Thiophenol, aniline, N-methylaniline, sodium phenoxide and sodium methoxide reacted with **1** to give 4-substituted products. On the other hand, Grignard reagents and alkyl amines afforded ring-opened products by nucleophilic attack at the 2-position. The difference in reaction position according to the kind of nucleophile can be reasonably interpreted in terms of the principle of hard and soft acids and bases. The "aromatic character" of thiopyrylium cation is discussed on the basis of the relative reactivities in nucleophilic substitution of **1**, N-methyl-4-chloropyridinium (**2**) and 4-chloropyrylium (**8**) cations.

Polymer Chemistry

Thin-Layer Chromatographic Separation of Polymers by the Difference in End-Group. T. I. Min, T. Miyamoto, and H. Inagaki. *Bull. Inst. Chem. Res., Kyoto Univ.*, **53**, 381 (1975).—The end-group effect upon polymer separation by thin-layer chromatography (TLC) is examined, using three types of polystyrenes without, and with one and two carboxyl end-groups. TLC experiments by the polarity-controlled adsorption mechanism indicated that complete separation was achieved according to such a slight change in the overall composition of sample as induced by the end-group. On the other hand, it was found that TLC experiments by the solubility-controlled phase-separation mechanism was inappropriate for the purpose.

Apparent Specific Volumes of Styrene-Methyl Methacrylate Copolymers of Varying Microstructure and Composition. A. Nakazawa, Y. Murakami, T. Kotaka, and H. Inagaki. *Bull. Inst. Chem. Res., Kyoto Univ.*, **53**, 387 (1975).—Apparent specific volumes of styrene-methyl methacrylate copolymers of varying architecture and composition were determined in *p*-xylene at $30.00 \pm 0.01^\circ\text{C}$. The results were compared with the theory of Inagaki which assumes the additivity of molar volumes of diads rather than of monomeric units. The experimental data are in agreement with the theory. The specific volumes of statistical copolymers can be described by those of the parent homopolymers and the alternating copolymer with the diad frequencies deduced from the copolymerization kinetics, while those of two

or three block copolymers are nearly the composition average of those of the parent homopolymers, since the contribution from the diads of unlike monomer units is negligible in such block polymer chains.

A 'Segregated' Conformation Model of AB-Diblock Copolymers. T. Tanaka, T. Kotaka, and H. Inagaki. *Bull. Inst. Chem. Res., Kyoto Univ.*, **54**, 91 (1976).—A hypothetical model representing the conformation of an AB-diblock copolymer chain was proposed. In the model the two blocks are spatially separated from each other by two parallel planes with the A-B junction point in between so as to form pure A, A-B intermixing and pure B phases. Dimensional parameters of the model were calculated on the basis of the random-flight statistics. It was found that the behavior of the model, which presumably constitute one extreme case of a real block copolymer chain, are qualitatively similar to those of our lattice-walk model proposed previously, and in a certain case they even show quantitative agreement.

Gel Permeation Chromatography: Band-Broadening and Skewing in High Speed Gel Permeation Chromatography. T. Kotaka, H. Suzuki, and H. Inagaki. *Bull. Inst. Chem. Res., Kyoto Univ.*, **54**, 100 (1976).—A computer simulation of gel permeation chromatographic (GPC) fractionation of polymers was carried out with introducing a simple skewed function as the band-spreading function. With the aid of these results as well as those of actual GPC experiments on narrow distribution polystyrenes, a phenomenological method was proposed for calibrating a GPC unit for band-broadening and skewing phenomena, which one often encounters on operating a high speed GPC. The performance of a high speed GPC was discussed in regard with such phenomena.

Determination of Compositional Heterogeneity of Styrene-Methyl Methacrylate Block Copolymers. T. Kotaka, T. Uda, T. Tanaka, and H. Inagaki. *Makromol. Chem.*, **176**, 1273 (1975).—Determinations of compositional heterogeneity of anionically prepared block copolymers of styrene (S) and methyl methacrylate (M) were attempted by three different methods: thin-layer chromatography (TLC), cross-fractionation, and by a computer simulation method. To this end the TLC elution behavior of diblock and triblock copolymers of SM- and MSM-type were compared with those of their statistical copolymers. A new TLC method was devised which does not require any reference samples as TLC elution standards. The compositional distributions determined by the three methods were in good agreement with one another, and found to be unexpectedly broad. The implication of such a result was discussed on the basis of the polymerization mechanism of the block copolymers.

Zur stereospezifischen Polymerisation von Methylmethacrylat mit Grignard-Reagens. T. Miyamoto, S. Tomoshige, und H. Inagaki. *Makromol. Chem.*, **176**, 3035 (1975).—The microstructure of poly(methyl methacrylate), (PMMA), prepared from methyl methacrylate with butylmagnesium chloride in toluene at -50°C in the absence (blank polymerization) and presence of preformed isotactic PMMA (replica polymerization), was studied.

In the blank polymerization, a relation was found between the microstructure of whole polymerization products and the conversion of monomer: the products obtained at lower conversions (<10%) were predominantly isotactic, and the isotacticity decreased with increasing conversion, approaching a constant value. Furthermore the acetone-insoluble fractions of the products were separated into components on a preparative scale by a competitive adsorption method. The triad isotacticity of isotactic components was remarkably high (ca. 85%), while the triad syndiotacticity of syndiotactic components was ca. 60–70%. The molecular weight of the syndiotactic components was considerably lower than that of the isotactic components. On the other hand, the acetone-soluble fractions were assigned to be "atactic" from their behavior in thin layer chromatography.

The polymerization products obtained by the replica polymerization, in sharp contrast with the products obtained by the blank polymerization, were predominantly syndiotactic, especially, when the mass ratio of produced polymer to added polymer was lower than ca. two. The difference between the two rates of polymerization was within the experimental error.

Compositional Heterogeneity and Molecular Weight: Distribution of Copolymer Systems, 2. T. Kotaka. *Makromol. Chem.*, **177**, 159 (1976).—The heterogeneity of graft copolymers was interpreted on the basis of the kinetics of free-radical grafting under the conditions in which grafting was expected to be random. Besides some well-known kinetic equations, a new equation relating the rate of graft-chain production with the initiator, monomer, and prepolymer concentrations was derived. The theory was applied to analyze Cameron's data on the benzoyl peroxide initiated styrene grafting onto polybutadiene in benzene. It was found that the theory quantitatively describes the experimental results. Also an equation relating the graft fraction with the prepolymer and monomer concentrations under the conditions in which terminations were dominated by disproportionation was proposed.

On the Structure of 3,4-*cis*-1,4-polyisoprene by ^{13}C n.m.r. W. Gronski, N. Murayama, H.-J. Cantow, and T. Miyamoto. *Polymer*, **17**, 358 (1976).—The ^{13}C n.m.r. spectrum of polyisoprene, prepared with $\text{Ti}(\text{O}-\text{C}_3\text{H}_7)_4\text{-Al}(\text{C}_2\text{H}_5)_3$ in toluene at 0°C, was investigated. The microstructure was found to be 1,4-*cis*-units=36% and 3,4-units=64%. Fine structures, due to different isomeric structures of neighboring units, were observed for the resonances of methylene C-atoms of *cis*-1,4- and 3,4-units and methine C-atoms of 3,4-units. The assignment indicated a tendency to alternating placement of 1,4-*cis*- and 3,4-units. The relative intensities of signals were analyzed by the first order Markov statistics with moderate success.

Thin-Layer Chromatographic Identification of Chain Architectures of Styrene-Butadiene Copolymers. N. Donkai, T. Miyamoto, and H. Inagaki. *Polymer Journal*, **7**, 577 (1975).—The feasibilities of thin-layer chromatography as a tool to identify the chain architecture of given copolymer samples have been investigated. To this end, styrene-butadiene (SB) block copolymers with known chain architecture were prepared and used as reference samples. Preliminary TLC ex-

periments on these samples indicated that the random, tapered, diblock and triblock SB-samples could be chromatographically distinguished from one another under suitable development conditions. By applying the procedures thus established, the chain architecture of various commercial SB-products could be identified without appreciable interference from the molecular weight and composition.

Hypochromic Effects in UV Spectra of Polymers in Solution. B. Stützel, T. Miyamoto, and H.-J. Cantow. *Polymer Journal*, **8**, 247 (1976).—The hypochromic effect in the UV spectra of polystyrene and styrene copolymers in solution was investigated in detail. For this purpose, isotactic and syndiotactic-rich polystyrenes as well as their dimer model compounds, 2,4-diphenylpentanes, and styrene-methyl methacrylate copolymers were prepared. UV absorption measurements were carried out in dioxane and tetrahydrofuran at various temperatures. The extinction coefficients of phenyl rings depended not only on the solvent and the temperature but also on the microstructure of the polymers. A discontinuous temperature dependence of the extinction coefficients was observed between 40 and 50°C for homopolystyrenes as well as their dimer model compounds. It was suggested that this might be explained in terms of the rotation of phenyl rings. On the other hand, the hypochromicity in binary copolymers appeared to depend strongly on the sequential arrangement of monomers (the chain architecture and the chemical composition of copolymers). The measured average extinction coefficients were well interpreted by a simple treatment by using triad probability proposed by Harwood. The results were discussed in relation to the UV spectrometer which is being used as an auxiliary detector in gel-permeation chromatography and microcolumn chromatography.

Ultracentrifuge Study of Critically Branched Polycondensates III. Sedimentation Equilibrium. M. Gordon, C. G. Leonis, and H. Suzuki. *Proc. R. Soc. Lond. A.*, **345**, 207 (1975).—Sedimentation-equilibrium experiments were performed on 2-butanone solutions of standard polystyrene (one sample) and polycondensates (five samples) obtained near the gel point of decamethylene glycol and benzene 1,3,5-triacetic acid stabilized afterwards by modification of the unreacted groups with diazomethane and ketene. The materials are known to deviate very little from the classical theory of polycondensation. The ordinary theory of plotting the reciprocal of apparent molecular mass M_1^{app} against the average concentration \bar{c} was successful for the standard polystyrene, because it has a narrow distribution with respect to molecular mass. For the polycondensates, however, the apparent molecular mass depends too strongly on rotor speed to extrapolate it reliably to infinite dilution. Two complementary ways for eliminating the dependence of M_1^{app} on rotor speed are proposed. Method (i): a plot of $(\bar{M}_1^{\text{app}})^{-1}$ against the generalized speed parameter λ , and method (ii): \bar{M}_1^{app} against $\Delta c^2/2(c^0)^2$, where Δc is the difference in concentration between the ends of a solution column and c^0 stands for the initial concentration. Both are successful for the polycondensates, giving the same results within experimental error. Method (i) is based on the theory of the asymptotic case $\lambda M_i \gg 1$ (where M_i is the molecular mass of component i) which is derived with

adequate rigour for dilute solutions of critically branched polycondensates, and it may be applicable more widely.

Solubilities of Inert Gases in Styrene-Butadiene-Styrene Block Copolymers. H. Odani, K. Taira, T. Yamaguchi, N. Nemoto, and M. Kurata. *Bull. Inst. Chem. Res., Kyoto Univ.*, **53**, 409 (1975).—The solubility coefficients of helium, argon, and xenon in two SBS block copolymer samples having different domain structures were determined between 25 and 120°C by the desorption and the time-lag methods. In the first method after the equilibrium had been established between polymer and gas phase, the dissolved gas was desorbed into a known large volume, and the solubility coefficient S was evaluated. In the second method the time-lag solubility coefficient S_θ was calculated from the values of permeability and (time-lag) diffusion coefficients, which were obtained from permeability experiments. In the desorption process of the first method, the pressure increase in the desorption system was measured as a function of time, and the diffusion coefficient was estimated therefrom. For all systems over the pressure and temperature range studied, Henry's law was always obeyed, and little differences between two copolymer samples were observed. At lower temperatures the values of S were greater than those of S_θ . It was concluded that the time-lag method counts only the mobile penetrant molecule in the rubbery polybutadiene matrix, while the desorption method counts less diffusive species in the glassy polystyrene domains as well. In the temperature region below about 85°C the temperature dependence of the solubility coefficient was expressed well by the Arrhenius-type equation with a constant apparent heat of solution. The diffusion coefficient estimated from the desorption method agreed practically with that evaluated from the time lag of permeability measurements. The relationship between the logarithm of S at 25°C and the Lennard-Jones force constant ϵ/k of the gases was well expressed by a straight line. Also, the apparent heat of solution was linearly correlated with ϵ/k . The slopes of the both plots were found to be well compared with those predicted by the thermodynamic treatment developed by Michaels and Bixler. The product of the tortuosity factor and the chain immobilization factor was estimated from the observed diffusion, permeation, and solubility coefficients. It was found that the products for the sample, in which polystyrene rods dispersed in polybutadiene matrix, were smaller than those for the other sample having domain structure of alternating lamellae of styrene and butadiene components. The products for the latter sample increased with increasing the molecular size of the gas.

Thermodynamic Analysis of Polymer-Mixed Solvent Systems. Part I. Osmotic Pressure and Theta Composition of Solvent. M. Kurata. *Bull. Inst. Chem. Res., Kyoto Univ.*, **54**, 112 (1976).—The osmotic equilibrium between polymer-mixed solvent system and dialyzate has been analyzed by using the characteristic function $F = A - \sum_{i=0}^d n_i \mu_i$ and the volume molality as composition variable. Here A is the Helmholtz free energy, n_i and μ_i are the amount and the chemical potential of diffusible components i ($=0, 1, \dots, d$). It is proved that at the theta composition of the dialyzate, the second virial coefficient of the polymer solution vanishes, and

simultaneously, the phase separation sets in if the polymer molecular weight is infinitely large. Thus, if the dialysis method is properly applied, the nature of the theta state in mixed solvent systems becomes exactly identical with that in single solvent systems.

Permeation, Diffusion, and Solution of Gases in SBS Block Copolymer Films. H. Odani, K. Taira, N. Nemoto, and M. Kurata. *Denki Kagaku (J. Electrochem., Ind. Phys. Chem.)*, **44**, 311 (1976), in Japanese.—The permeation, diffusion, and solution behavior for a series of inert gases in SBS block copolymer films were studied at temperatures from 25 to 120°C by transient permeability measurements and by the equilibrium desorption method. The domain structures of the sample films, assured by electron microscopic observation, were (a) polystyrene rods dispersed in polybutadiene matrix, and (b) alternating lamellae of styrene and butadiene components. The inert gases used were helium, argon, nitrogen, krypton, and xenon. The temperature dependence of permeability, diffusion, and solubility coefficients at temperatures between 25 and 75°C was represented by the Arrhenius-type equation with constant activation energies of permeation and diffusion and heat of solution, respectively. It was concluded that the transient method counts only the mobile gas molecules in the rubbery polybutadiene matrix, while the equilibrium method counts less diffusive species as well. The observed values of permeability coefficient for the block copolymer films were well explained in terms of a simple model consisting of a parallel array of elements of the respective component homopolymers. The diffusion behavior was discussed in terms of two impedance factors: tortuosity and chain immobilization factors.

Nonlinear Viscoelasticity of Polystyrene Solutions. I. Strain-Dependent Relaxation Modulus. M. Fukuda, K. Osaki, and M. Kurata. *J. Polym. Sci.: Polym. Phys. Ed.*, **13**, 1563 (1975).—Strain-dependent relaxation moduli $G(t, s)$ were measured for polystyrene solutions in diethyl phthalate with a relaxometer of the cone-and-plate type. Ranges of molecular weight M and concentration c were from 1.23×10^6 to 7.62×10^6 and 0.112 to 0.329 g/cm³. Measurements were performed at various magnitudes of shear s ranging from 0.055 to 27.2. The relaxation modulus $G(t, s)$ always decreased with increasing s and the relative amount of decrease (i.e., $-\log[G(t, s)/G(t, 0)]$) increased. However, the detailed strain dependences of $G(t, s)$ could be classified into two types according to the M and c of the solution. When $cM < 10^6$, the plot of $\log G(t, s)$ versus $\log t$ varied from a convex curve to an S-shaped curve with increasing s . For solutions of $cM > 10^6$, the curves were still convex and S-shaped at very small and large s , respectively, but in a certain range of s (approximately $3 < s < 7$) $\log G(t, s)$ decreased rapidly at short times and then very slowly; a peculiar inflection and a plateau appeared on the plot of $\log G(t, s)$ versus $\log t$. The strain-dependent relaxation spectrum exhibited a trough at times corresponding to the plateau of $\log G(t, s)$. The longest relaxation time $\tau_1(s)$ and the corresponding relaxation strength $G_1(s)$ were evaluated through the "Procedure X" of Tobolsky and Murakami. The relaxation time $\tau_1(s)$ was independent of s for all the solutions studied while $G_1(s)$ decreased with s . The reduced relaxation strength $G_1(s)/G_1(0)$ was a simple function of s (The plot of $\log G_1(s)/G_1(0)$ against $\log s$ was a convex curve)

and was approximately independent of M and c in the range of $cM < 10^6$. This behavior of $G_1(s)/G_1(0)$ was in agreement with that observed for a polyisobutylene solution and seems to have wide applicability to many polymeric systems. On the other hand, $\log G_1(s)/G_1(0)$ as a function of $\log s$ decreased in two steps and decreased more rapidly when M or c was higher. It was suggested that in the range of $cM < 10^6$, a kind of geometrical factor might be responsible for a large part of the nonlinear behavior, while in the range of $cM > 10^6$, some "intrinsic" nonlinearity of the entanglement network system might be important.

Nonlinear Viscoelasticity of Polystyrene Solutions. II. Non-Newtonian Viscosity. K. Osaki, M. Fukuda, S. Ohta, B. S. Kim, and M. Kurata. *J. Polym. Sci.: Polym. Phys. Ed.*, **13**, 1577 (1975).—The steady shear viscosity $\eta(\kappa)$ and the stress decay function $\eta(t, \kappa)$ (the shear stress divided by the rate of shear κ after cessation of steady shear flow) were measured for concentrated solutions of polystyrene in diethyl phthalate. Ranges of molecular weight M and concentration c were 7.10×10^5 to 7.62×10^6 and 0.112 – 0.329 g/cm³, respectively. Measurements were performed with a rheometer of the cone-and-plate type in the range $10^{-4} < \kappa < 1$ sec⁻¹. The Cox-Merz relation $\eta(\kappa) = |\eta^*(\omega)|_{\omega=\kappa}$ was tested with the experimental result ($|\eta^*(\omega)|$ is the magnitude of the complex viscosity). It was found to be applicable to solutions of relatively low M or c but not to those of high M and c . For the latter $\eta(\kappa)$ began to decrease at a lower rate of shear than $|\eta^*(\omega)|_{\omega=\kappa}$ did; the Cox-Merz law underestimated the effect of rate of shear. The stress decay function was assumed to have a functional form $\eta(t, \kappa) = \sum \eta_p(\kappa) e^{-t/\tau_p(\kappa)}$ where $\tau_1 > \tau_2 > \dots$, and the values of τ_1 , τ_2 , η_1 , and η_2 were determined for some solutions. The relaxation times τ_1 and τ_2 were found to be independent of κ and equal to the relaxation times of linear viscoelasticity. At the limit of $\kappa \rightarrow 0$, η_1 and η_2 were approximately 60 and 20–30%, respectively, of η and the non-Newtonian behavior was due to large decrease of η_1 and η_2 with increasing κ . It was shown that $\eta_1(\kappa)$ may be evaluated from the relaxation strength $G_1(s)$ for the longest relaxation time of the strain-dependent relaxation modulus with a constitutive model for relatively high c - M systems as well as for low c - M systems.

Concentration Dependences of Nonlinear Viscoelastic Functions for Polystyrene Solutions. M. Fukuda, K. Osaki, and M. Kurata. *J. Soc. Rheol., Japan*, **3**, 114 (1975), in Japanese.—Concentration dependences of viscoelastic functions $G(t, s)$, $\eta(t, \kappa)$, and $\eta(t, \kappa)$ were examined on solutions of two polystyrenes ($M_w = 3.10 \times 10^6$ and 5.53×10^6) in diethyl phthalate. Here G is the relaxation modulus, s is the magnitude of shear, and $\kappa\eta$ and $\kappa\eta$ are shear stresses after the start and cessation, respectively, of steady shear flow with the rate of shear κ . When the concentration c was relatively low, i.e., when $cM_w < 10^6$ g/cm³, the reduced functions $\bar{\eta}/\eta^0$ and η/η^0 obtained at various c were unique functions of two reduced variables t/τ_1^0 and $\kappa\tau_1^0$. Here η^0 is the zero shear viscosity and τ_1^0 is the longest relaxation time. The reduced function G/G_1^0 , where G_1^0 is the relaxation strength corresponding to τ_1^0 , was also a unique function of two variables, t/τ_1^0 and s , in the same range of c as above. In this case, however, a slight dependence of G/G_1^0 on c remained uneliminated.

nated at relatively short times. These results may indicate that in the description of nonlinear viscoelastic effect, the strain rate is most properly expressed in reference to the rate of stress relaxation $1/\tau_1^0$. This method of reduced variables was not applicable when the concentration was higher than the values stated above.

Rheology of Copolymer Solutions. I. The Viscosity and the Transient Stresses at the Start and Cessation of Steady Shear Flow for a Solution of SBS Block Copolymer. B. S. Kim, K. Osaki, and M. Kurata. *J. Soc. Rheol., Japan*, **4**, 16 (1976), in Japanese.—Transient shear stresses, $\kappa\bar{\eta}(t, \kappa)$ and $\kappa\bar{\eta}(t, \kappa)$, at a sudden start and cessation, respectively, of steady shear flow were measured for a 20% solution of styrene-butadiene-styrene triblock copolymer in cetyl chloride. Here κ is the rate of shear, t the time, η the stress development function, and η the stress decay function. Measurements were performed with a rheometer of the cone-and-plate type in the range $5 \times 10^{-4} < \kappa < 7 \text{ sec}^{-1}$ at 15.8°C and at every 5°C interval starting from 20°C up to 40°C. A polystyrene of molecular weight close to that of polystyrene blocks precipitated from solution when the temperature was decreased below 30°C. Results on $\eta(t, \kappa)$ indicated that the contribution from relaxation modes of long relaxation times selectively decreased with increasing rate of shear. The method of reduced variables with respect to κ and the temperature T was not applicable to the steady shear viscosity $\eta(\kappa)$ below 30°C. The Cox-Merz empirical law concerning $\eta(\kappa)$ and the complex viscosity was not applicable also in the same range of T . These results may be due to destruction of structures formed by precipitated polystyrene blocks in solution below 30°C.

Rheology of Copolymer Solutions. II. The Strain-Dependent Relaxation Modulus and the Constitutive Equation. K. Osaki, B. S. Kim, N. Bessho, and M. Kurata. *J. Soc. Rheol., Japan*, **4**, 21 (1976), in Japanese.—The strain-dependent relaxation modulus $G(t, s)$ was measured for a 20% solution of styrene-butadiene-styrene triblock copolymer in cetyl chloride at 15.8 and 20°C. Measurements were performed with a cone-and-plate relaxometer in the range of shear $0.222 \leq s \leq 6.68$. The strain-dependent relaxation spectrum $H(\tau, s)$ obtained from $G(t, s)$ indicated that the relaxation mode of the longest relaxation time was very sensitive to shear and decreased rapidly in the strain range $0.5 < s < 1.0$. The applicability of the strain-dependent constitutive model (or the BKZ model) was examined: The memory function was obtained from $G(t, s)$ and therefrom were calculated the steady shear viscosity and the transient shear stresses at a sudden start and cessation, respectively, of steady shear flow. Calculated results were in good agreement with the experimental results given in part I.

Viscoelastic Properties of Polymer Solutions in High-Viscosity Solvents and Limiting High-Frequency Behavior. III. Poly(2-substituted methyl acrylates).¹ J. W. M. Noordermeer, J. D. Ferry, and N. Nemoto. *Macromolecules*, **8**, 672 (1975).—The storage (G') and loss (G'') shear moduli were measured for dilute solutions of four poly(2-substituted methyl acrylates) in two Aroclors with the modified Birnboim transducer. The substituents were methyl, ethyl, *n*-butyl, and phenyl.

The molecular weights of the samples were between 6.5×10^4 and 2.85×10^6 . The range of concentration was 0.73×10^{-2} to 4.28×10^{-2} g/ml and the temperatures were between 8.3 and 43.8°C. The frequency range was 0.25 to 630 Hz. Data at different temperatures for G' and $G'' - \omega\eta_s$, where ω is the radian frequency and η_s the solvent viscosity, were successfully combined by the method of reduced variables with a reference temperature of 25°C. The intrinsic dynamic viscosity at high frequency, $[\eta']_\infty$, is independent of the molecular weight for each polymer, but differs among the various polymers: poly(methyl methacrylate) 22.8 ml/g; poly(methyl-2-ethyl acrylate) 18.5 ml/g; poly(methyl-2-*n*-butyl acrylate) 13.3 ml/g; and poly(methyl-2-phenyl acrylate) 18.5 ml/g. A comparison of these results with former data on polystyrene and poly(α -methylstyrene) can be made; all these polymers have the vinyl group as the backbone supporting unit. The contributions to the high-frequency viscosity per monomer unit may then be interpreted in terms of the types of substitution of this vinyl group. They increase when the monomer substitution changes from single aromatic, through double aliphatic, to mixed aliphatic-aromatic. For the sufficiently monodisperse samples the frequency dependence of G' and G'' could be described by the Peterlin internal viscosity theory. On basis of the experimental results the latter theory is compared with more recent theories on the dynamic viscoelastic behavior of dilute polymer solutions.

Studies on the Structure of Filamentous Bacteriophage fd II. All-or-None Disassembly in Guanidine-HCl and Sodium Dodecyl Sulfate. K. Ikehara, H. Utiyama, and M. Kurata. *Virology*, **66**, 306 (1975).—Equilibrium properties and kinetics of the disassembly of coliphage fd induced by guanidine hydrochloride and sodium dodecyl sulphate were investigated by means of uv absorption, circular dichroism, and sedimentation. In both cases the phage disassembled in an all-or-none fashion, and the concentrations of the midtransition were 6.4 M and 0.03%, respectively, at 25°. The dissociation of the minor coat protein and the loss of infectivity were ascertained to take place in the disassembly. The DNA and major coat protein molecules released in guanidine hydrochloride solutions were both in nearly random coil conformations. In the sodium dodecyl sulphate disassembly the dissociated DNA molecule exhibited the same uv absorption as in the intact phage, and the dissociated major coat protein molecule remained in an approximately 50% α -helical conformation.

Studies on the Structure of Filamentous Bacteriophage fd III. A Stable Intermediate of the 2-Chloroethanol-Induced Disassembly. K. Ikehara and H. Utiyama. *Virology*, **66**, 316 (1975).—By incubation of bacteriophage fd at 25° for 20 hr in 15% (v/v) 2-chloroethanol, 0.14 M NaCl, 0.02 M Tris, pH 7.6, we obtained a stable defective particle lacking the minor coat protein (A-protein) and infectivity. The defective particle could not be distinguished from the intact phage by measurements of uv absorption, circular dichroism, sedimentation velocity, and CsCl buoyant density. The melting temperature of the defective particle as determined by the midtransition of the uv absorption at 260 nm in 4 M guanidine hydrochloride, 0.14 M NaCl, 0.02 M Tris, pH 7.6, was about 2.5° lower than that of the intact phage.

An Apparatus for Measuring Flow-Induced Crystallization of Polymers. K. Katayama, S. Murakami, and K. Kobayashi. *Bull. Inst. Chem. Res., Kyoto Univ.*, **54**, 82 (1976).—Requirements of an apparatus for measuring flow-induced crystallization of polymers were discussed on the basis of a nonisothermal crystallization theory. Results of calculation with a computer indicated that the thickness of a specimen with relatively large heat of crystallization should be less than 0.05 mm to observe rapid crystallization process which would complete in, say, one second. Then, a special apparatus was designed and constructed to fulfill the requirements. With this apparatus, it was possible to heat a thin polymer specimen between beryllium plates (50 μ thick) above its melting point, quench the specimen to a crystallization temperature, and then deform the supercooled specimen by loading one of the beryllium plates with a weight. The process of crystallization was observed by X-ray method, and the displacement of the plate was recorded by means of a differential transformer. From these data, we obtained the degree of crystallinity and the shear strain as functions of time. Some results of the flow-induced crystallization of a polyethylene (Sholex 6009) were also illustrated.

Comments on the Morphology of Polymers Crystallized from Oriented Melts. T. Amano, S. Kajita, and K. Katayama. *Progr. Colloid & Polymer Sci.*, **58**, 108 (1975).—Molecular orientation due to melt flow has a profound effect on the nature of subsequent crystallization from the melt. This resulting crystalline morphology was examined with a polarizing microscope to understand the cases intermediate between quiescent melts on the one hand and highly oriented melts on the other. It seems unlikely that fibrillar nucleation along extended molecules occurs in general. Rather a more satisfactory picture is one in which the dominant orientation-dependent factor is a restriction of the lamellar growth to certain directions. This mechanism is emphasized as opposed to the concept of a direction-dependent growth rate or the earlier concept of fibrillar nucleation. A picture developed along these lines allows one to explain the entire spectrum of structure, ranging from spherulites of the one hand to "stacked lamellar" structure on the other.

Biochemistry

Studies on Bacteriophage fd DNA. III. Nucleotide Sequence Preceding the RNA Start-Site on a Promoter-Containing Fragment. K. Sugimoto, H. Sugisaki, T. Okamoto, and M. Takanami. *Nucleic Acid Research*, **2**, 2091 (1975).—A short DNA fragment containing a strong promoter was isolated from phage fd replicative form DNA with the use of restriction endonucleases, and the sequence of 110 nucleotides in the region preceding the RNA start-site was determined. The sequence was: (5') CGGTCTGGTTCGCTTTGAGGCTCGAATTAACGCG-ATATTTGAAGTCTTTCGGGCTTCCTCTTAATCTTTTGTATGCAATTGCG-TTTGCTTCTGACTATAATAGACAGG (3').

Sequence of Promoter for Coat Protein Gene of Bacteriophage fd. M. Takanami, K. Sugimoto, H. Sugisaki, and T. Okamoto. *Nature*, **260**, 297 (1976).—

The nucleotide sequence in the promoter region for the coat protein gene of phage fd has been determined. This sequence contains an endonuclease R-Hha cleavage site at the fifteenth nucleotide upstream from the RNA start site. Cleavage results in loss of promoter function. Comparison with the sequence of another fd promoter indicates that the longest sequence common to both was TATAAT in the region in which RNA polymerase forms a stable initiation complex.

Effect of Glutamine Analogs on Glutaminase Formation in *Pseudomonas aeruginosa*. M. Ohshima, T. Yamamoto, and K. Soda. *Bull. Inst. Chem. Res., Kyoto Univ.*, **54**, 170 (1976).—The bacterial distribution of glutaminase activities was investigated with the cell-free extracts. Glutaminase activity was found in all the strains tested. The cell-free extract of *Pseudomonas aeruginosa* possesses the highest activity. The production of glutaminase was examined by adding glutamine analogs to the medium. The substrates and products of glutaminase reaction stimulated the production of glutaminase. L-Glutamine and L-asparagine were the most effective inducers.

Biological Activity of *Hansenula jadinii* with Regard to Large Scale Fermentative Production of CDP-Choline. (Phosphorylation of Choline and CMP and Inhibition of Choline Kinase by CTP.) Y. Kariya, K. Aisaka, A. Kimura, and T. Tochikura. *Bull. Inst. Chem. Res., Kyoto Univ.*, **54**, 183 (1976).—Fructose 1,6-bisphosphate was more favorable energy source than glucose for the phosphorylation of both choline and CMP and for CDP-choline formation under fermentative conditions. In the reaction system using FBP as energy source, the yield of CDP-choline at an early stage of incubation was much higher than that of glucose, and phosphorylation rate of both CMP and choline was several times larger than in the glucose system. Under the fermentative conditions used here, phosphorylation of a small amount of CMP did not compete with the phosphorylation of choline for their energy requirement, but in the reaction mixture which contained more than 40 mM of CTP, the rate of CDP-choline formation was considerably decreased. *Hansenula jadinii* exhibited high activity of phosphorylation of CMP to CTP under fermentative conditions. More than 40 mM of CMP were phosphorylated within 2 hr incubation by 100 mg per ml of the dried cells and the product CTP was stable on further incubation. Activity of choline phosphorylation was lower than that of CMP phosphorylation. The ratio of choline phosphorylation to CMP phosphorylation was calculated as 1/10 to 1/5 on the rate of ATP consumption. *H. jadinii* exhibited high inorganic pyrophosphatase activity. Two hundred and forty mM of inorganic pyrophosphates were hydrolyzed by one mg of cells per hr. Choline phosphorylation was inhibited by high concentration of CTP, and inhibition of choline kinase by CTP was confirmed with purified choline kinase. An improved method for CDP-choline in high yield from CMP and choline was investigated. By feeding small amounts of CMP and glucose successively to the reaction mixture, the concentration of CTP accumulated in the reaction mixture could be maintained below the levels at which choline kinase was inhibited. By this method, more than 33 mM of CDP-choline was produced from the final concentration of 50 mM of CMP. In-

hibition of choline kinase by CTP was investigated by use of purified choline kinase. Aminoethanols were phosphorylated by this yeast under the condition of glucose catabolism.

Bacterial Metabolism of Lysine Analogues. H. Tanaka and K. Soda. *Bull. Inst. Chem. Res., Kyoto Univ.*, **53**, 284 (1975).—*Aerobacter aerogenes* was found capable of growing well in the medium containing *S*-(β -aminoethyl)-L-cysteine as a sole nitrogen source. The main metabolic products from *S*-(β -aminoethyl)-L-cysteine have been isolated, purified and identified as *S*-(β -*N*-acetyl-aminoethyl)-L-cysteine and *S*-(β -*N*-acetyl-aminoethyl)- α -keto-mercaptopropionate. The terminal amino group of *S*-(β -aminoethyl)-L-cysteine is acetylated by acetyltransferase to yield *S*-(β -*N*-acetyl-aminoethyl)-L-cysteine, and then the acetylated compound is readily deaminated by L-amino acid oxidase to form the corresponding α -keto acid, *S*-(β -*N*-acetyl-aminoethyl)- α -keto-mercaptopropionate.

The enzyme catalyzing the first step, *S*-(β -aminoethyl)-L-cysteine ω -*N*-acetyltransferase has been purified about 450-fold from the cell-free extract of *A. aerogenes* grown in the *S*-(β -aminoethyl)-L-cysteine-peptone medium. The purified enzyme is homogeneous by the criterion of disc gel electrophoresis, and has an approximate molecular weight of 100,000. The optimum pH is at about 8.0. The following lysine analogues were prepared to investigate substrate specificity of the enzyme; *S*-(β -aminoethyl)-L-cysteine hydroxamate, *S*-(β -aminoethyl)-L-cysteine-*dl*-sulfoxide and sulfone, *S*-(β -aminoethyl)-mercaptopropionate and *S*- β -(2-pyridylethyl)-L-cysteine. In addition to *S*-(β -aminoethyl)-L-cysteine, its D-enantiomer, sulfoxide, sulfone, and a higher homologue, and an oxygen analogue of lysine, *O*-(β -aminoethyl)-DL-serine act as acetyl acceptors. L- or D-Lysine and L- or D-ornithine also can accept an acetyl group to a certain extent, but α - or ω -acetylated derivatives of both *S*-(β -aminoethyl)-L-cysteine and L-lysine are not active. Acetyl-CoA is the exclusive acyl donor in the transfer reaction. The Michaelis constants were determined as follows; *S*-(β -aminoethyl)-L-cysteine, 2.1×10^{-3} M, *S*-(β -aminoethyl)-D-cysteine, 1.6×10^{-3} M, *O*-(β -aminoethyl)-DL-serine, 1.7×10^{-3} M, *S*-(β -aminoethyl)-L-homocysteine, 7.1×10^{-4} M, and acetyl-CoA, 4.5×10^{-3} M. The enzyme activity is inhibited competitively by propionyl-CoA, butyryl-CoA and benzoyl-CoA against acetyl-CoA. *S*-(β -aminoethyl)-mercaptopropionate and *S*-(β -aminoethyl)- α - β -*N*-acetyl-L-cysteine are strong competitive inhibitors of *S*-(β -aminoethyl)-L-cysteine acetylation. The enzyme catalyzing the second step has been shown to be an L-amino acid oxidase, which occurs widely in bacteria.

Occurrence of Kynurenine Aminotransferase in Extracts of Yeasts. K. Yonaha, M. Moriguchi, T. Hirasawa, T. Yamamoto, and K. Soda. *Bull. Inst. Chem. Res., Kyoto Univ.*, **53**, 315 (1975).—The activity of kynurenine aminotransferase was investigated in various strains of yeasts. The aminotransferase occurs in several strains of yeasts. Kynurenine aminotransferase was partially purified from *Hansenula schneggii* in which the enzyme was found most abundantly. The enzyme had the maximum reactivity at about pH 8.2. Michaelis constants for L-Kynurenine and α -ketoglutarate were determined as 2.2 mM and 5 mM, respectively. Amino acceptor

specificity was investigated with kynurenine and various keto acids. The following relative activities were obtained; 100, 90, 6, and 53, for α -ketoglutarate, pyruvate, oxalacetate, and glyoxylate, respectively. The enzyme was inhibited 40% by D-cycloserine (1 mM), and 75% by hydroxylamine (1 mM), which are the typical inhibitors for pyridoxal 5'-P enzymes. Pyridoxal 5'-P partially reversed the inhibition by the reagents. The aminotransferase was also inhibited about 33% by adipate.

CDP-Choline Production from CMP and Choline by Yeasts. Y. Kariya, A. Kimura, and T. Tochikura. *Bull. Inst. Chem. Res., Kyoto Univ.*, **53**, 546 (1975).—Fermentative production of CDP-choline by yeast from choline and CMP by a choline kinase-linked system was investigated. Yeasts having marked activity of CDP-choline formation and choline phosphorylation were sought. *H. jadinii* was selected as a suitable strain of CDP-choline forming yeast. Other than *H. jadinii*, *C. utilis* IFO 0396, IFO 0639, IFO 1086, *H. beijerinckii* IFO 0981, *H. miso* IFO 0146, *S. carlsbergensis* IFO 0641, *S. cerevisiae* IFO 0021, *S. rouxii* IFO 0320 and IAM 4369 showed comparable activity of CDP-choline formation. CDP-choline production by *H. jadinii* was strictly controlled by pH of the reaction mixture, CMP concentration, phosphate ion concentration and cultivation time of the cells. When the pH of the initial reaction system was lower than 6.5, CDP-choline formation was remarkably reduced. Long time cultivation of cells resulted in significant reduction in the activity of both choline kinase and CDP-choline-cytidyl transferase. The phosphorylation of CMP was not affected by long time cultivation. Under higher concentration of phosphate ions than 4×10^{-1} M, the rate of glucose dissolution gradually fell and caused decrease of CMP phosphorylation. The optimum condition were as follows: CMP, 20 mM; choline, 80 mM; potassium phosphate (pH 8.0), 300 mM; glucose, 600 mM; $\text{MgSO}_4 \cdot 7\text{H}_2\text{O}$ 30 mM; and dried cells 100–200 mg per ml in a total volume of 2.0 ml. More than 13 mM of CDP-choline was produced under the optimum condition. The method presented in this paper will be developed to provide easy production of ^{32}P -labeled or ^{14}C -labeled CDP-choline and other CDP-aminoethanols.

Enzymological Properties of Bacterial D-Amino Acid Aminotransferase. K. Yonaha, H. Misono, and K. Soda. *Amino Acid and Nucleic Acid.*, **32**, 34 (1975), in Japanese.—D-Amino acid aminotransferase of *Bacillus sphaericus* IFO 3525 was purified about 970-fold. The purification was carried out by the following steps: Sonic extraction, protamine sulfate treatment, ammonium sulfate fractionation, DEAE-cellulose column chromatography, hydroxyapatite column chromatography and Sephadex G-150 gel filtration. The purified enzyme was crystallized by addition of ammonium sulfate. The crystals took the form of fine needles. The crystalline enzyme was shown to be homogeneous by the criteria of ultracentrifugation and disc gel electrophoresis. The sedimentation coefficient (s , w) of the enzyme was 4.30S. The enzyme has a molecular weight of about 60,000 and consists of two subunits identical in molecular weight (30,000). The enzyme exhibits absorption maxima at 280, 330, and 415 nm, which are independent of the pH (5.5–10.0), and contains two moles of pyridoxal 5'-phosphate per mole of enzyme. One of them absorbing at 415 nm is bound in an aldimine linkage to the ϵ -amino group of lysine residue of the protein, and

released by incubation with phenylhydrazine to yield the catalytically inactive form. The inactive form, which is reactivated by addition of pyridoxal 5'-phosphate, has still a 330 nm peak and contains one mole of pyridoxal 5'-phosphate. Therefore, this form is regarded as a semiapoenzyme. The holoenzyme shows the negative circular dichroic bands at 330 and 415 nm. D-Amino acid aminotransferase catalyzes α -transamination of various D-amino acid and α -keto acids. D-Alanine D- α -aminobutyrate and D-glutamate, and α -ketoglutarate, pyruvate and α -ketobutyrate are the preferred amino donors and acceptors, respectively. The enzyme activity is significantly affected by both the carbonyl and sulfhydryl reagents. The Michaelis constants are follows: D-alanine (1.3 and 4.2 mM with α -ketobutyrate and α -ketoglutarate, respectively), α -ketobutyrate (1.4 mM with D-alanine), α -ketoglutarate (3.4 mM with D-alanine), pyridoxal 5'-phosphate (2.3 μ M with D-alanine- α -ketoglutarate transamination) and pyridoxamine 5'-phosphate (25 μ M with D-alanine- α -ketoglutarate transamination).

Fermentative Production of CDP-Choline and Related Cytidine Coenzymes by Dried Cells of Yeasts. A. Kimura, Y. Kariya, K. Aisaka, and T. Tochikura. *Amino Acids and Nucleic Acids*, **33**, 1 (1976).—CDP-choline and CDP-ester of aminoethanols were produced under the condition of yeast fermentation. The mechanism of the reaction was composed of two different systems. One was phosphorylation of CMP and aminoethanols by use of energy of yeast fermentation, and the other was condensation of CTP and phosphorylated aminoethanols.

There important conditions were necessary for the fermentative production of cytidine coenzymes: 1) water content of yeast have to be lowered below than 30%, 2) presence of high levels of phosphate ions, 3) suitable concentration of glucose and CMP.

Intact cells of yeast could not phosphorylate CMP and could not form CDP-choline. Treatment of intact cells by triton X-100 was effective to phosphorylate CMP and to produce CDP-choline.

Fermentative Production of CDP-Choline Analogues by *Hansenula jadinii*. Y. Kariya, K. Aisaka, Y. Kaji, A. Kimura, and T. Tochikura. *Amino Acids and Nucleic Acids*, **33**, 4 (1976).—CDP-choline analogues were produced from CMP and choline analogues, N-substituted aminoethanols, with a dried cell preparation of *Hansenula jadinii* IFO 0987 by a fermentative process under a choline kinase-linked system. The yields of CDP-dimethylaminoethanol and CDP-diethylaminoethanol were comparable to that of CDP-choline; that of CDP-dimethylaminoethanol was somewhat higher. The yield of CDP-ethanolamine was as low as 20% of that of CDP-choline, even when phosphoryl ethanolamine was used instead of ethanolamine. The CDP-choline pyrophosphorylase in *H. jadinii* was active toward most phosphate esters of N-substituted aminoethanols, but not toward phosphorylethanolamine to form CDP-ethanolamine.

An elevated concentration of mono-, and dimethylaminoethanol inhibited glucose catabolism, aminoethanol phosphorylation and CDP-ester formation. Crystalline preparations of the sodium salt of both CDP-dimethylaminoethanol and CDP-diethyl-

aminoethanol were prepared and characterized by chemical and physicochemical procedures.

Microbial Assimilation of Alkyl Nitro Compounds and Formation of Nitrite. T. Kido, T. Yamamoto, and K. Soda. *Amino Acid Nucleic Acid*, **33**, 24 (1976), in Japanese.—Representative 66 strains of bacteria, yeasts, and fungi were tested for their ability to grow in a semidefined medium containing 0.5% nitroethane as a nitrogen source. About half of them were found capable of growing in the medium. *Hansenula mrakii*, *Hansenula beijerinckii*, *Candida utilis* and *Penicillium chrysogenum* were most active in assimilating nitroethane. 2-Nitropropane inhibited growth of most of microorganisms tested in a medium containing 0.2% peptone and 0.2% glycerol. *H. mrakii* was found to grow rapidly in the nitroethane-peptone medium after a lag phase. Nitrite was accumulated in the culture fluid after the phase of logarithmic multiplication, and increased with increase of the growth, followed by a decline after the maximum growth. The alkyl nitro compounds were oxidatively denitrified to form nitrite by the crude enzyme from *H. mrakii*. Nitroethane was generally the poor substrate, but was the best inducer to produce the nitro compounds oxidizing enzyme. 2-Nitropropane and nitroethane were enzymatically oxidized to nitrite, and acetone and acetaldehyde, respectively, which were isolated as 2,4-dinitrophenylhydrazones and identified. Nitrite formed was found to be reduced into ammonia by the intact cells and also the crude enzyme.

Purification and Crystallization of Bacterial Aspartate Transaminase. T. Yagi, M. Toyosato, and K. Soda. *Amino Acid Nucleic Acid*, **33**, 45 (1976), in Japanese.—Aspartate aminotransferase was purified to homogeneity and crystallized from *Pseudomonas striata*. The molecular weight is approximately 80,000 ($s_{20,w}^0=4.2S$). The enzyme exhibits absorption maxima at 280 and 355 nm and at 440 nm at pH 8.0 and 6.0, respectively. The enzyme has a maximum reactivity at about pH 8.5 and catalyzes the transamination of glutamate, aspartate, cysteinesulfinate, phenylalanine, tyrosine and α -aminoadipate with α -ketoglutarate.

Effect of Sulfur Analogue of Lysine on Bacterial Protein Biosynthesis. H. Tanaka and K. Soda. *Amino Acid Nucleic Acid*, **33**, 87 (1976), in Japanese.—S-(β -Aminoethyl)-L-cysteine, a sulfur analogue of lysine inhibited strongly growth of *Escherichia coli* A-19, and weakly that of *Corynebacterium* sp. isolated from soil, but did not inhibit growth of *Aerobacter aerogenes*. In *Corynebacterium* sp. the inhibitory effect was markedly enhanced in the presence of L-threonine. The inhibition of growth by S-(β -aminoethyl)-L-cysteine was rapidly reversed by the addition of L-lysine.

S-(β -Aminoethyl)-L-cysteine inhibited protein synthesis and the activity of lysyl-tRNA synthetase from *E. coli* and *A. aerogenes*. All the other lysine analogues tested inhibited the activity of enzyme, but S-(β -aminoethyl)-L-cysteine derivatives, S-(β -N-acetylaminoethyl)-L-cysteine and S-(β -aminoethyl)- α -N-acetyl-L-cysteine were not effective.

Bacterial Metabolism of S-(β -Aminoethyl)-L-cysteine. H. Tanaka and

K. Soda. *Amino Acid Nucleic Acid*, **33**, 93 (1976), in Japanese.—The bacterial metabolism of the lysine sulfur analogue, *S*-(β -aminoethyl)-L-cysteine by *A. aerogenes* has been studied using *S*-labeled compound. In addition to *S*-(β -*N*-acetyl-aminoethyl)-L-cysteine previously reported, *S*-(β -*N*-acetyl-aminoethyl)- α -ketomercaptopropionate was identified as a metabolite of *S*-(β -aminoethyl)-L-cysteine. The results indicate that the terminal amino group of *S*-(β -aminoethyl)-L-cysteine is acetylated by acetyltransferase to yield *S*-(β -*N*-acetyl-aminoethyl)-L-cysteine and then the acetylated compound is readily deaminated by L-amino acid oxidase to form the corresponding α -keto compound, *S*-(β -*N*-acetyl-aminoethyl)- α -ketomercaptopropionate.

Alanine Racemase of *Bacillus subtilis* var. *aterrimus*. K. Yonaha, T. Yorifuji, T. Yamamoto, and K. Soda. *J. Ferment. Technol.*, **53**, 579 (1975).—Alanine racemase of *Bacillus subtilis* var. *aterrimus* was purified approximately 1,000-fold. The molecular weight was determined to be 60,000 by a Sephadex G-150 gel filtration. The enzyme is exclusively specific for alanine ($K_m=8.0$ mM). The following L-amino acid are inert; serine, phenylalanine, tyrosine, tryptophan, α -amino-*n*-butyrate, isoleucine, leucine, valine, arginine, ornithine, histidine, glutamate, aspartate, proline, and threonine. Glycine, and L- α -amine-*n*-butyrate inhibit the enzyme, and the other amino acids do not affect on the racemization of alanine. The enzyme has an optimum reactivity in the pH range of 9.0–9.5 and is most stable at pH 8.3. The enzyme shows an absorption maximum at 420 nm and is inhibited by carbonyl reagents. The activity is partially restored by addition of pyridoxal 5'-phosphate, suggesting that the enzyme requires pyridoxal 5'-phosphate as a cofactor. Flavin compounds have no effect on the enzyme activity. The enzyme is inhibited by most of the sulfhydryl reagents, and L-alanine, glycine and L- α -amino-*n*-butyrate protect the enzyme from the inhibition. It is likely that a sulfhydryl group plays an important role in the catalytic action. Both the conversion of D-alanine to L-alanine and the reverse are remarkably inhibited by D-penicillamine, but only slightly by the L-enantiomer.

Fermentative Production of CDP-Choline Analogues by *Hansenula jadinii*. Y. Kariya, K. Aisaka, Y. Kaji, A. Kimura, and T. Tochikura. *J. Ferment. Technol.*, **53**, 599 (1975).—CDP-choline analogues were produced from CMP and choline analogues, *N*-substituted aminoethanols, with a dried cell preparation of *Hansenula jadinii* IFO 0987 by a fermentative process under a choline kinase-linked system. The yields of CDP-dimethylaminoethanol and CDP-diethylaminoethanol were comparable to that of CDP-choline; that of CDP-dimethylaminoethanol was somewhat higher. The yield of CDP-ethanolamine was as low as 20% of that of CDP-choline, even when phosphoryl ethanolamine was used instead of ethanolamine. The CDP-choline pyrophosphorylase in *H. jadinii* was active toward most phosphate esters of *N*-substituted aminoethanols, but not toward phosphorylethanolamine to form CDP-ethanolamine.

An elevated concentration of mono-, and dimethylaminoethanol inhibited glucose catabolism, aminoethanol phosphorylation and CDP-ester formation. Crystalline preparations of the sodium salt of both CDP-dimethylaminoethanol and CDP-

diethylaminoethanol were prepared and characterized by chemical and physico-chemical procedures.

Reconstitution of D-Amino Acid Aminotransferase. K. Yonaha, H. Misono, and K. Soda. *FEBS Letters*, **55**, 265 (1975).—The reconstitution of enzyme with pyridoxal 5'-phosphate (PLP) was followed by spectrophotometry and determination of the enzyme activity. Both the Schiff base formation and the reconstitution of enzyme follow first order kinetics with half-times of about 2 and 20 min, respectively, suggesting that the reconstitution of D-amino acid transaminase with PLP proceed in at least three steps: a reversible association of semiapoenzyme with PLP, a Schiff base formation and a slow conformation change as follows.

PLP

Semiapoenzyme \rightleftharpoons complex I \longrightarrow complex II (Schiff base) \longrightarrow Active holoenzyme

Four sulfhydryl groups were titrated with DTNB in the holoenzyme, whereas only two groups were reactive in the semiapoenzyme. The semiapoenzyme treated with DTNB was reactivated almost fully by PLP. A Schiff base formation is not concurrently accompanied with a reappearance of reactivity of the sulfhydryl groups participating in catalysis with DTNB. The sulfhydryl groups become susceptible to DTNB in the last step.

Crystalline Aspartate Aminotransferase from *Pseudomonas striata*. T. Yagi, M. Toyosato, and K. Soda. *FEBS Letters*, **61**, 34 (1976).—Aspartate aminotransferase was purified by Ammonium sulfate fractionation, DEAE-cellulose, sephodex G-200 and Hydroxyapatite column chromatography and crystallization from the cell-free extract of *Pseudomonas striata*. The crystalline enzyme was shown to be homogeneous by the criteria of ultracentrifugate and disc gel electrophoresis. The sedimentation coefficient (S_{20}^0 , w) and molecular weight were determined to be 4.2 S and 80,000, respectively. The enzyme exhibits absorption maxima at 280, 355 nm at pH 8.0 and 280 and 440 nm at pH 6.0. The spectral shift of the enzyme by varying the pH is closely similar to that of the mammalian enzyme. The enzyme has a maximum reactivity in the pH range of 8.3–8.6 and catalyzes the transamination of glutamate, aspartate, cystinesulfinate, phenylalanine, tyrosine and α -aminoadipate with α -ketoglutarate.

Purification and Properties of Methioninase from *Pseudomonas ovalis*. H. Tanaka, N. Esaki, T. Yamamoto, and K. Soda. *FEBS Letters*, **66**, 307 (1976).—Methioninase was purified to homogeneity by DEAE-cellulose column chromatography, heat treatment and hydroxyapatite, DEAE-Sephadex A-50 and Sephadex G-200 column chromatography from the cell-free extract of *Pseudomonas ovalis*. The molecular weight is approximately 180,000 (S_{20}^0 , w=8.5 S). The enzyme exhibits absorption maxima at 278 and 420 nm. No appreciable spectral shifts occurred on varying the pH. In addition to L-methionine, which is the preferred substrate, several derivatives of L-methionine and L-cysteine, e.g., L-ethionine, DL-methionine sulfone, L-homocysteine and S-methyl-L-cysteine serve as the effective substrates. S-methyl-L-methionine and L-cysteine can be decomposed though slowly, whereas D-methionine,

D-cysteine and L-norleucine are inert. The enzyme has the maximum reactivity at about pH 8.0 for all the substrates.

Phosphorylation of Mononucleotides and Formation of Cytidine 5'-Diphosphate-Choline and Sugar Nucleotides by Respiration-Deficient Mutants of Yeasts. A. Kimura, K. Hirose, Y. Kariya, and S. Nagai. *J. Bacteriol.*, **125**, 744 (1976).—Respiration-deficient mutants (Rho⁻, petite) of *Saccharomyces carlsbergensis* were obtained by treatment with tryptaflavin (euflavine). Dried cells of these mutants phosphorylated mononucleotides to their triphosphates and further formed not only cytidine 5'-diphosphate-choline, but also sugar nucleotides, such as uridine 5'-diphosphate-glucose, guanosine 5'-diphosphate-mannose, etc. The activities were the same or slightly greater than those of the wild strain. These results showed that energy (adenosine 5'-triphosphate) necessary for phosphorylation of mononucleotides was sufficiently supplied by the glycolysis system.

Purification and Properties of Nitroalkane-Oxidizing Enzyme from *Hansenula mrakii*. T. Kido, T. Yamamoto, and K. Soda. *J. Bacteriol.*, **126**, 1261 (1976).—A nitroalkane-oxidizing enzyme was purified about 1,300-fold from a cell extract of *Hansenula mrakii* grown in a medium containing nitroethane as the sole nitrogen source by ammonium sulfate fractionation, diethylaminoethyl-cellulose column chromatography, hydroxyapatite column chromatography, and Bio-Gel P-150 column chromatography. The enzyme was shown to be homogeneous upon acrylamide gel electrophoresis and ultracentrifugation. The enzyme exhibits absorption maxima at 274, 370, 415, and 440 nm and a shoulder at 470 nm. Balance studies showed that 2 mol of 2-nitropropane is converted into an equimolar amount of acetone and nitrite with the consumption of 1 mol of oxygen. Hydrogen peroxide is not formed in the enzyme reaction. In addition to 2-nitropropane, 1-nitropropane and nitroethane are oxidatively denitrified by the enzyme, but nitromethane is inert to the enzyme. The nitroalkanes are not oxidized under anaerobic conditions.

D-Amino Acid Aminotransferase of *Bacillus sphaericus* Enzymologic and Spectrometric Properties. K. Yonaha, H. Misono, T. Yamamoto, and K. Soda. *J. Biol. Chem.*, **250**, 6983 (1975).—D-Amino acid aminotransferase, purified to homogeneity and crystallized from *Bacillus sphaericus*, has a molecular weight of about 60,000 and consists of two subunits identical in molecular weight (30,000). The enzyme exhibits absorption maxima at 280, 330, and 415 nm, which are independent of the pH (5.5 to 10.0), and contains 2 mol of pyridoxal 5'-phosphate per mol of enzyme. One of the pyridoxal-5'-P, absorbing at 415 nm, is bound in an aldimine linkage to the ϵ -amino group of a lysine residue of the protein, and is released by incubation with phenylhydrazine to yield the catalytically inactive form. The inactive form, which is reactivated by addition of pyridoxal 5'-phosphate, still has a 330 nm peak and contains 1 mol of pyridoxal 5'-phosphate. Therefore, this form is regarded as a semiapoenzyme. The holoenzyme shows negative circular dichroic bands at 330 and 415 nm. D-Amino acid aminotransferase catalyzes a transamination of various D-amino acids and α -keto acids. D-Alanine, D- α -aminobutyrate and D-

glutamate, and α -ketoglutarate, pyruvate, and α -ketobutyrate are the preferred amino donors and acceptors, respectively. The enzyme activity is significantly affected by both the carbonyl and sulfhydryl reagents. The Michaelis constants are as follows: D-alanine (1.3 and 4.2 mM with α -ketobutyrate and α -ketoglutarate, respectively), α -ketobutyrate (14 mM with D-alanine), α -ketoglutarate (3.4 mM with D-alanine), pyridoxal 5'-phosphate (2.3 μ M) and pyrisoxamine 5'-phosphate (25 μ M).

Microbial Assimilation of Alkyl Nitro Compound and Formation of Nitrite. T. Kido, T. Yamamoto, and K. Soda. *Arch. Microbiol.*, **106**, 165 (1975).—*Abstract.* 66 representative strains of bacteria, yeasts and fungi were tested for their ability to grow in a semidefined medium containing 0.5% nitroethane as a nitrogen source. About half of them were found capable of growing in the medium. *Hansenula beijerinckii*, *Candida utilis*, and *Penicillium chrysogenum* were most active in assimilating nitroethane. 2-Nitropropane inhibited growth of most of the microorganisms tested in a medium containing 0.2% peptone and 0.2% glycerol. *Hansenula mrakii* was found to grow rapidly in the nitroethane-peptone medium after a lag phase. Nitrite was accumulated in the culture fluid after the phase of logarithmic multiplication, and increased with increase of the growth, followed by a decline after the maximum growth. The alkyl nitro compounds were oxidatively denitrified to from nitrite by the crude enzyme from *Hansenula mrakii*. Nitroethane was generally a poor substrate, but was the best inducer to produce the nitro compounds oxidizing enzyme. 2-Nitropropane and nitroethane were enzymatically oxidized to nitrite, and acetone and acetaldehyde, respectively, which were isolated as 2,4-dinitrophenylhydrazones and identified. Nitrite formed was found to be reduced into ammonia by the intact cells and also the crude enzyme.

Amino Acid Dehydrogenase of Bacilli: The Enzymological Properties and Antitumor Activity. K. Soda. *Kagaku to Seibutsu*, **14**, 379 (1976).—Distribution, cofactor requirement, the enzymological and physicochemical properties, and the antitumor activity of amino acid dehydrogenases of Bacilli were described. The physiological functions of the enzymes were also discussed here.

An Assay Method of Taurine-Pyruvate Transaminase Activity with 2,4-Dinitrophenylhydrazine. S. Toyama, M. Yasuda, and K. Soda. *Ryukyus Daigaku Nogakubu Gakkujutsu Hōkoku (The Sci. Bull. Coll. Agr., The Univ. of Ryukyus)*, **22**, 215 (1975), in Japanese.—A new assay procedure of taurine-pyruvate transaminase with 2,4-dinitrophenylhydrazine was established. 2,4-Dinitrophenylhydrazine was added to the enzyme reaction mixture to yield hydrazones. After separation of the hydrazones with toluol, to the aqueous layer containing sulfoacetaldehyde hydrazone was added the alkaline solution, and the red color produced was measured at 435 nm. The linear relationship was observed between absorbance and the amount of enzyme or the incubation time.

Enzymatic Conversion of S-(β -N-Acetyl-aminoethyl)-L-cysteine into Its α -Keto Analogue. H. Tanaka and K. Soda. *Agr. Biol. Chem.*, **40**, 441 (1976).—

When $[S^{35}]\text{-S-(}\beta\text{-acetyl-aminoethyl)-L-cysteine}$ was incubated with resting cells or a crude enzyme of *Aerobacter aerogenes*, oxygen uptake was observed and formation of two unknown radioactive compounds were demonstrated by high-voltage paper electrophoresis in 0.25 M pyridine-acetate buffer (pH 4.8). These compounds were termed tentatively compounds A and B in the order of these increasing mobilities. Both compounds were not visualized with ninhydrin but with a platinum reagent. Only compound A reacted with 2,4-dinitrophenylhydrazine to form the hydrazone. Both compounds A and B were isolated. Compound A was identified as, *S*-(β -*N*-acetyl-aminoethyl)- α -ketomercaptopropionate by paper chromatography and paper electrophoresis. The findings suggest that *S*-(β -acetyl-aminoethyl)-L-cysteine was oxidatively deaminated to form the α -keto analogue by an oxidase. Compound B did not react with ninhydrin and 2,4-dinitrophenylhydrazine, but did with a platinum reagent, and moved toward the anode electrophoretically. Therefore, compound B is probably *S*-(β -*N*-acetyl-aminoethyl)- α -hydroxymercaptopropionate or the closely related compound as postulated for lysine metabolism of *Neurospora* and *Hansenula saturnus*.

Unidirectional Stability of α -Helix. Theoretical Calculation and Attempt for Synthesis of Block Copolypeptides. T. Kontani, K. Nishikawa, T. Iio, S. Takahashi, and T. Ooi. *Bull. Inst. Chem. Res., Kyoto Univ.*, **54**, 128 (1976).—The stability of α -helical structure in the *N*-terminal half and the *C*-terminal half of the helix, was investigated when the distortion was brought about at the middle of the chain. Calculation was carried out on two parameters, $\Delta\tau$ and ΔE , which represent the difference of the *i*-th rotational angle of peptide plane around the *i*-th virtual bond and that of the energy of the *i*-th residue between the distorted conformation and the standard α -helix respectively. The results showed that both of the two values were convergent to zero along the *C*-terminal direction, but amplified in the *N*-terminal direction. We attempted to synthesize (glu)₂₀(ala)₂₀, and (ala)₂₀(glu)₂₀, which would offer experimental evidences for the results of the calculation to be justified, with a general method of solid-phase peptide synthesis. It revealed, however, that the method was unable to afford the desired products, because the yield of (glu)_n and (ala)_n were gradually decreased with increasing *n*. The practical limit of *n* was found to be approximately 10.

Disulfide Bond Formation during Renaturation of Bovine Pancreatic Ribonuclease A. Biochemical Assignments of Location of Cystinyl Residues in the Intermediate Protein Species and Theoretical Considerations on the Folding Pathway. S. Takahashi and T. Ooi. *Bull. Inst. Chem. Res. Kyoto Univ.*, **54**, 141 (1976).—The order of disulfide formation of four cystinyl residues in bovine pancreatic ribonuclease A during renaturation was studied. Protein intermediates were quenched by carboxymethylation at several stages of renaturation, digested with proteolytic enzymes, and analyzed by column chromatography for cystine-containing peptides. Analysis showed that random disulfides formed at the initial stage were reshuffled to specific cysteine pairs in the following sequence. Cys 58, 65, and 72 were most rapid to give specific systines, then Cys 84 followed. These experimental evidences understood as one of the two wings observed in the three di-

mensional structure of the native RNase A is generate at first. Almost all the available data on renaturation of RNase A support this folding scheme. Theoretical basis in favor of the Assigned folding pathway was also given.

Similarities and Differences of the α and β Components of Tropomyosin. N. Ookubo, H. Ueno, and T. Ooi. *J. Biochem.*, **78**, 739 (1975).—Rabbit skeletal tropomyosin was separated into two components by CM cellulose column chromatography in the presence of urea. The two components are different from TN-T, since upon addition of the components to F-actin solutions, they increase the degree of flow birefringence while TN-T does not, and the reduced mean residue ellipticities at 220 nm are about 2.5 fold higher than for TN-T. The two components are not identical for the following reasons; 1) leucine is the C-terminus of the one chain, and isoleucine is that of the other., 2) the former has a lower helicity, and 3) the former has a higher content of glutamic acid and methionine than the latter. The Electron micrographs of the paracrystals of both components show a band pattern with 400 Å periodicity.

Properties of Non-Polymerizable Tropomyosin Obtained by Carboxypeptidase A Digestion. H. Ueno, Y. Tawada, and T. Ooi. *J. Biochem.*, **80**, 283 (1976).—Tropomyosin digested with carboxypeptidase A shows a lower viscosity than the undigested protein in solution. From the relation between the viscosity decrease and the amount of amino acids liberated from the C-terminus during this digestion, it is inferred that loss of the tripeptide -Thr-Ser-Ile from the C-terminus is responsible for the decrease in viscosity. The secondary structure was not affected by the digestion according to CD measurements.

A decrease in the viscosity of tropomyosin solutions was observed on the addition of CTM, indicating the CTM interacts with intact tropomyosin. The dependence of the viscosity decrease on the amount of CTM showed that CTM binds tropomyosin in a one-to-one ratio as a result of end-to-end interaction.

The disc gel electrophoretic pattern showed that troponin could bind to CTM, but no increase in viscosity due to the complex was observed in solution. That is, the C-terminus region of tropomyosin is not required for the formation of the complex.

Geometrical Criteria for Formation of Coiled-Coil Structures of Polypeptide Chains. K. Nishikawa and H. A. Scheraga. *Macromolecules*, **9**, 395 (1976).—Crick's general formulas describing a coiled coil are expressed in a different form to combine the parameters of a coiled coil with the backbone dihedral angles of a polypeptide chain, assuming that the bond lengths and bond angles of the chain are fixed. While the existence of a low-energy coiled-coil conformation depends on energetic considerations, these formulas, which pertain to single-stranded structures and, by application of symmetry operations, to multistranded structures, provide the geometrical criteria for the existence of coiled coils. The concept of "the averaged structure of the minor helix", introduced here, makes it possible to relate the shape of the major helix to that of the minor helix. It is shown, in the analysis of a simple model of a single-stranded coiled-coil β structure, that strong geometrical restrictions

exist for the formation of coiled-coil structures from a given minor helix conformation of a polypeptide chain; these restrictions are expressed in a general form that is applicable to any coiled-coil of any number of residues in a repeat unit. As an application, the possible existence of a two-stranded coiled-coil antiparallel β structure is considered, both geometrically and energetically, and discussed in relation to the observed twisted β structures in globular proteins. The proposed coiled-coil models of α -helical proteins are also examined briefly.